CHEMISTRY
A EUROPEAN JOURNAL

DOI: 10.1002/chem.200601186

Fullerene-Derivatized Amino Acids: Synthesis, Characterization, Antioxidant Properties, and Solid-Phase Peptide Synthesis

Jianzhong Yang, Lawrence B. Alemany, Jonathan Driver, Jeffrey D. Hartgerink, and Andrew R. Barron*[a]

Abstract: A series of [60]fullerene-substituted phenylalanine (Baa) and lysine derivatives have been prepared by the condensation of 1,2-(4′-oxocyclohexano)fullerene with the appropriately protected (4-amino)phenylalanine and lysine, respectively. Conversion of the imine to the corresponding amine is achieved by di-acid catalyzed hydroboration. The reduction of the imine is not accompanied by hydroboration of the fullerene cage. The [70]fullerene phenylalanine derivative has also been prepared as have the di-amino acid derivatives. The compounds were characterized by MALDI-TOF mass spectrometry, UV/Vis spectroscopy, and cyclic voltammetry. ^{1}H and ^{13}C NMR spectroscopy allowed the observation of diastereomers. Fullerene-substituted peptides may be synthesized on relatively large scale by solid-phase peptide synthesis. The presence of the C_{60}-substituted amino acid in a peptide has a significant effect on the secondary structures and self-assembly properties of peptides as compared to the native peptide. The antioxidant assay of Baa and a Baa-derived anionic peptide was determined to be significantly more potent than Trolox.

Keywords: amino acids · antioxidant · fullerenes · peptides

Introduction

Since fullerenes were discovered in 1985[1] finding practical applications of these novel materials has been a major area of research. Although initial commercial applications are rather mundane with low impact, applications in biological sciences have been seen as the archetype of combining wet and dry nanotechnologies.[2] One reason for the interest in the incorporation of fullerene into macromolecular structures with biological importance is the highly hydrophobic nature and unusual physicochemical properties of fullerenes, making them ideal candidates as interesting pharmocophores. Unfortunately, the direct use of fullerenes in biological applications is limited by their poor solubility in aqueous media.[3] To overcome this obstacle, two different approaches have been adopted to increase the solubility. The first strategy involves non-covalently encapsulating fullerene molecules into soluble polymeric or host molecules.[4–6] The second strategy relies on covalent functionalization of fullerene by introduction of hydrophilic groups by chemical modification.[7] The latter approach is attracting more interest as it can not only alter the physical and chemical properties of fullerene to readily achieve desired properties, but it can also provide useful building blocks for further molecular constructions. It is this latter approach that has piqued our interests due to the potential of using a fullerene-based amino acid derivative for the systematic creation of nano-bio conjugates using traditional peptide synthesis approaches.

Amino acids are the most basic and essential building unit for living organisms at all levels. The incorporation of fullerene-based amino acids into proteins, peptides or antibodies could lead to new applications in medicinal chemistry. The possible interaction of fullerenes with hydrophobic pockets or arene–arene interactions within protein or enzymes could provide new insights in the function and structure study of those proteins and enzymes. Thus, the functionalization of [60]fullerene (C_{60}) as an amino acid analogue and its incorporation into a peptide is desirable, especially with regard to targeted interactions. To date, several approaches have been taken towards synthesizing fullerene-based amino acids.[8–13] All of these compounds are derived from aliphatic amino acids and commonly employ ester or amide linkages. In contrast, an additional requirement of our general synthetic ap-

[a] J. Yang, Dr. L. B. Alemany, J. Driver, Prof. J. D. Hartgerink, Prof. A. R. Barron
Richard E. Smalley Institute for Nanoscale Science and Technology
The Institute of Biosciences and Bioengineering, and
Center for Biological and Environmental Nanotechnology
Rice University, Houston, Texas 77005 (USA)
Fax: (+1) 713-348-5619
E-mail: arb@rice.edu

proach was the presence of a stable (non-hydrolyzable) linkage (e.g., an amine versus an amide or ester) to enable solid-phase peptide synthesis (SPPS). In this regard, we have previously reported the synthesis of an arene-based amino acid, Bucky amino acid (Baa, **1a**) along with its N-Boc protected derivative (N-Boc-Baa, **1b**; N-Boc = *N*-butyloxycarbonyl).[14] We have also reported the uptake and interaction of Baa with human epidermal keratinocytes (HEK).[15] MTT cell viability after 48 h significantly decreased for concentrations of 0.4 and 0.04 mg mL^{-1}. In an additional study, human cytokines were assessed for exposure to Baa, and our results indicate that for concentrations of less than 0.04 mg mL^{-1} cell viability is maintained.

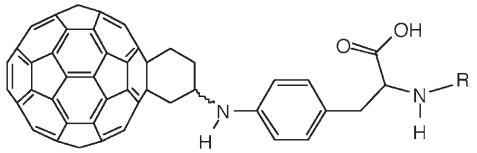

R = H (Baa, **1a**); C(O)O*t*Bu (N-Boc-Baa, **1b**)

One of the goals in the development of a fullerene amino acid with a linkage group not susceptible to hydrolysis was to provide an easily adapted route to a wide range of fullerene amino acids and derivatives. A further goal was to demonstrate the application of the fullerene amino acid in SPPS. In this regard, we report herein the synthesis of a range of fullerene amino acid derivatives and related compounds along with a demonstration of SPPS. We also explore the properties of Baa and its peptide derivatives with regard to cell toxicity.

Results and Discussion

Fullerene amino acids and related derivatives: We have previously communicated[14] that ester protected-Baa and N-Boc-Baa may be prepared by the condensation of 1,2-(4′-oxocyclohexano)fullerene[16,17] with ester- or Boc-protected (4-amino)phenylalanine, $H_2NC_6H_4CH_2CH(COR^1)(NHCOR^2)$ (Scheme 1, where R^1 = OMe, R^2 = Me; R^1 = OH, R^2 = Me, O*t*Bu). Conversion of the imine to the corresponding amine is achieved by di-acid catalyzed hydroboration.[14] Reaction of the N-Ac amino ester with BBr_3 leads to the formation of the parent amino acid. The 9-fluorenylmethoxycarbonyl derivative (Fmoc-Baa, **1c**) can also be prepared in an analogous manner. In each case the imine and amine derivatives can be isolated and characterized (see below).

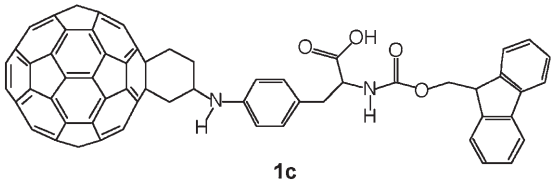

1c

As a route to determining the effects of the rigid phenyl linkage (between the α-amino acid moiety and the C_{60}), as opposed to a flexible linkage, we have prepared lysine-derivatized fullerene amino acids (**2**–**4**) using the same approach (see Experimental Section). It should be noted that the yields are significantly lower than the phenylalanine ana-

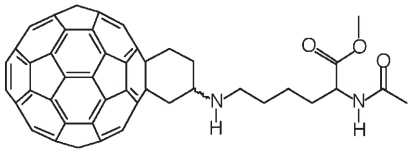

2

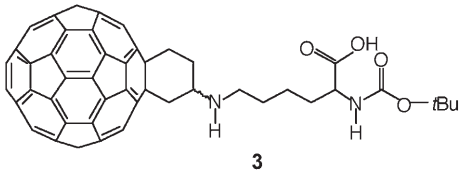

3

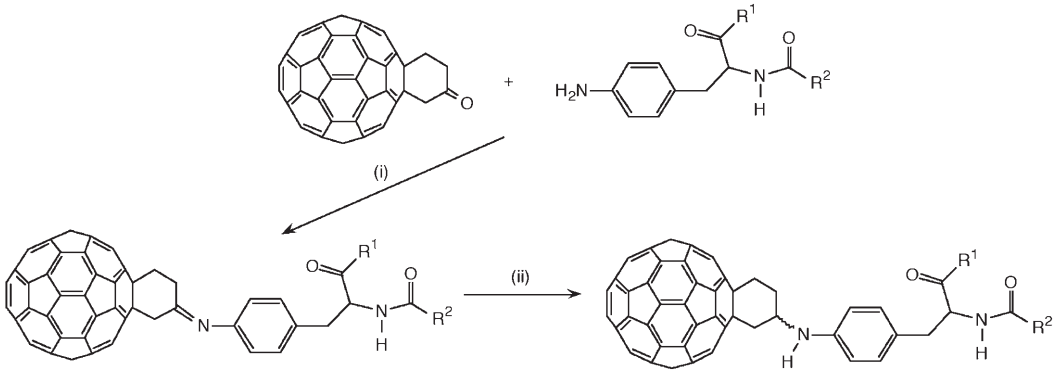

R^1 = OMe, R^2 = Me (**1**)
R^1 = OH, R^2 = O*t*Bu (**3**)

R^1 = OMe, R^2 = Me (**2**)
R^1 = OH, R^2 = O*t*Bu (**4**)

Scheme 1. Synthesis of protected fullerene-based amino acids: i) toluene reflux, ii) BH_3·THF at −78 °C.

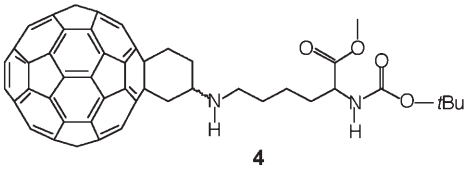

4

logues (see Experimental Section); however, the generality of the condensation of 1,2-(4′-oxocyclohexano)fullerene with an aniline derivative allows the general high-yield synthesis of a wide range of substituted C_{60} derivatives, that is, compounds **5**–**8** (see Experimental Section).

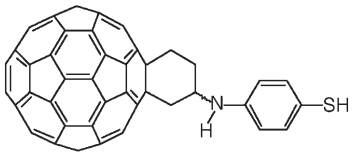

5

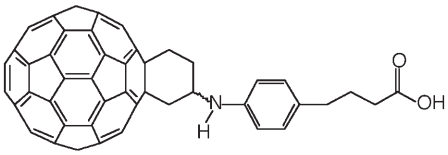

6

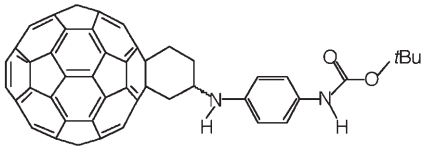

7

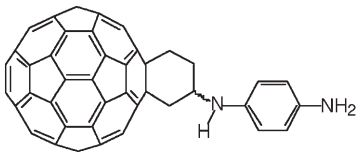

8

We have previously noted that during the synthesis of 1,2-(4′-oxocyclohexano)fullerene the di-ketone derivative (**9**) may also be formed as a mixture of isomers.[14] Isolation of **9** allows for the synthesis of bi-functional fullerene compounds (**10** and **11**).

Evidence for the formation of fullerene amino acid derivatives was confirmed by MALDI-TOF mass spectrometric

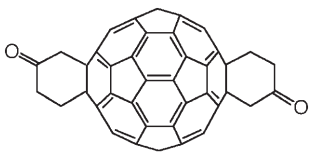

9

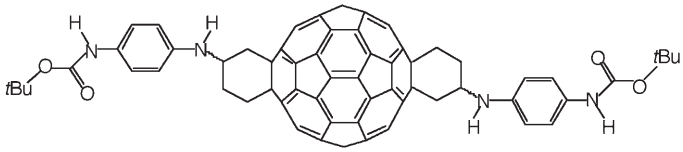

10

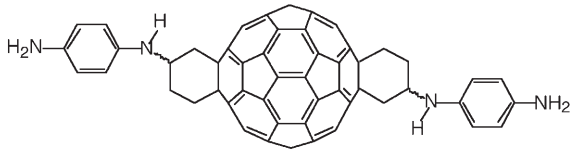

11

analysis. The molecular ion peaks for all fullerene derivatives can be readily observed with sulfur as the matrix and the instrument operating in the linear mode. The quality of the spectrum is further improved by using sulfur as the matrix. Molecular ion peaks, together with signals due to fragmentation, were clearly observed in all of the mass spectra of new compounds (see Experimental Section).

As reported previously,[14] the electronic absorption properties of each of the fullerene amino acids and derivatives are very similar to that of unfunctionalized C_{60}. The only minor difference is that fullerene mono-adducts show a small weak transition around 430–450 nm, a characteristic peak of C_{60} mono-adducts; this weak transition disappears in bis-adducts.

The electrochemical behavior of C_{60} fullerene amino acids (N-Boc-Baa **1b** and Fmoc-Baa **1c**) was determined by cyclic voltammetry (CV) in solutions of DMF/toluene (3:2) at room temperature with $[Bu_4N][BF_4]$ as the electrolyte. The distinctive features of the cyclic voltammograms for both of the protected fullerene amino acids are the close similarity to that of pristine C_{60},[18,19] which implies that the fullerene core remains intact during the synthesis process (Figure 1). Interestingly, four couples of reversible redox waves are observed in the accessible potential window of the solvent

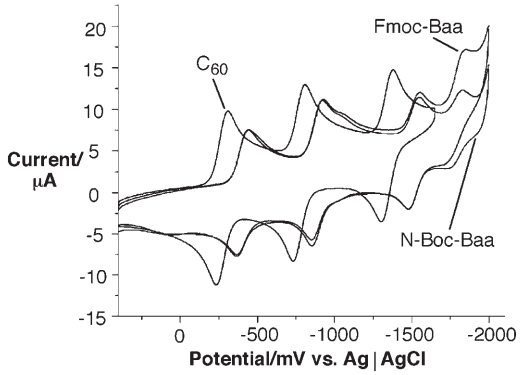

Figure 1. Cyclic voltammograms of C_{60}, N-Boc-Baa and Fmoc-Baa in 0.1 M TBA$[BF_4]$ in DMF/toluene (3:2) at room temperature. Scan rate, 100 mV s^{-1}.

under the present conditions for N-Boc-Baa **1b** and Fmoc-Baa **1c** in contrast to only three waves shown for pristine C_{60}. Detailed redox potential data are summarized in Table 1. No well-defined reversible redox waves were observed in the positive potential region. The three well-defined redox waves (I, II, and III in Table 1) observed for all listed compounds shift toward more negative potentials relative to unfunctionalized C_{60}. This trend is due to the decrease of p delocalization on the fullerene cage as a consequence of the introduction of two sp^3 carbon atoms. The CV profiles of protected fullerene amino acids clearly show the potential of using fullerene amino acids as antioxidants (see below).

Table 1. Cyclic voltammetry of Baa derivatives.

Compound	Formal potential,[a] $E_{1/2}$			
	I	II	III	IV
C_{60}	−0.271	−0.771	−1.342	
N-Boc-Baa	−0.402	−0.888	−1.513	−1.797
Fmoc-Baa	−0.406	−0.891	−1.517	−1.806

[a] Formal potentials are calculated as averages of oxidation and reduction peak potentials. Potentials are given in volts versus a reference electrode, Ag|AgCl.

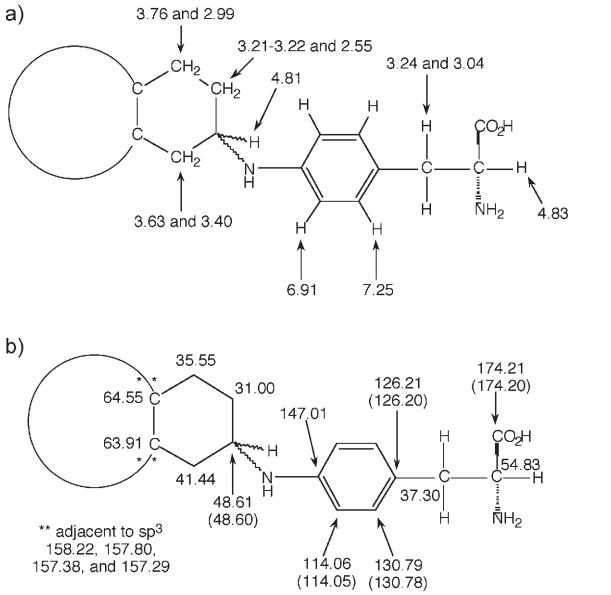

Figure 2. Assignment of a) ^{1}H and b) ^{13}C NMR spectra for Baa (**1a**). ^{13}C peaks due to second diastereomer are given in parentheses. [For these pairs of signals, it is not obvious which signals are from the (*R*,*S*) diastereomer and which are from the (*S*,*S*) diastereomer.]

NMR characterization of Baa derivatives: 1D and 2D NMR spectroscopic analyses provide detailed and crucial information that establish the molecular structures of the fullerene amino acid derivatives. Fortunately, most fullerene amino acid derivatives are sufficiently soluble for NMR analysis, but multiple attempts at finding the best solvent system are generally required to achieve maximum concentration. A mixed-solvent system significantly interrupts the intermolecular aggregation between fullerene compounds; however, the signal overlap in the alkyl regions somewhat limits spectral assignments at 500 MHz. The NMR spectra of Baa (**1a**), N-Boc-Baa (**1b**), and Fmoc-Baa (**1c**) were assigned from a combination of 1D ^{1}H, ^{13}C, and DEPT-135 ^{13}C experiments and, for **1a** and **1c**, 2D ^{1}H–^{1}H COSY, ^{1}H–^{13}C HSQC, and ^{1}H–^{13}C HMBC experiments. NMR chemical shift assignments for **1a** and **1c** are given in Figure 2 and Figure 3.

The ^{1}H NMR signals for the CH_2 groups of the cyclohexyl rings in both N-Boc-Baa (**1b**) and Fmoc-Baa (**1c**) are well resolved even at room temperature. Clearly the introduction of the phenylalanine moiety increased the energy barrier of the inversion of the cyclohexyl ring as compared to the bucky ketone. Given the highly complex nature of the spectra it is worth noting that the two diastereomers, formed as a consequence of the achiral hydrogenation (see Scheme 1), are readily observed in the ^{13}C experiment (Figure 2 and Figure 3).

Figure 2 shows the ^{1}H and ^{13}C NMR assignments for the diastereomeric mixture (*R*,*S*) and (*S*,*S*) of Baa (**1a**). For a given diastereomer, the inequivalence of the protons within each methylene group is apparent. The analysis is complicated by multiplets from protons in two different methylene groups extensively overlapping at about $\delta = 3.22$ ppm and by multiplets from the two aliphatic methine protons extensively overlapping at about $\delta = 4.82$ ppm. For the two diastereomers, any slight difference in the ^{1}H chemical shift of a given proton is not recognized at 500 MHz with a digital resolution of 0.20 ppb. The chemical shifts of the phenylalanine CH_2 protons and the phenylalanine aromatic protons in the two diastereomers should be the most sensitive to the stereochemistry because these protons are between the two chiral centers. However, only four signals (not eight signals for two diastereomers) are resolved for each phenylalanine CH_2 proton (the four A signals and the four B signals of the phenylalanine CH_2-CH ABX spin system), and only two signals (not four signals for two diastereomers) are resolved for each phenylalanine aromatic proton (the two A signals and the two X signals of the phenylalanine aromatic AX spin system). For reference, we note that in the two diastereomers of 1,2-bis(2-ethylhexyl)phthalate, the chemical shifts of the inequivalent OCH_2 protons in one diastereomer differ from those in the other diastereomer by 1.5 ppb.[20] In compound **1a**, the two chiral centers are much further apart than in this phthalate, and thus it is not surprising that the chemical shifts of corresponding protons in the diastereomers of compound **1a** differ by much less than 1.5 ppb.

In contrast to the ^{1}H NMR spectrum, the shift differences for the two diastereomers are recognizable in the ^{13}C spectrum, as most of the carbons near one chiral center or between the two chiral centers give a pair of signals of essentially equal intensity differing in chemical shift by 8–16 ppb (digital resolution = 0.76 ppb) (Figure 4). That such pairs of signals are observed is not surprising since ^{13}C chemical shifts are known to be very sensitive to remote changes in stereochemistry.[21] The presence of essentially equal

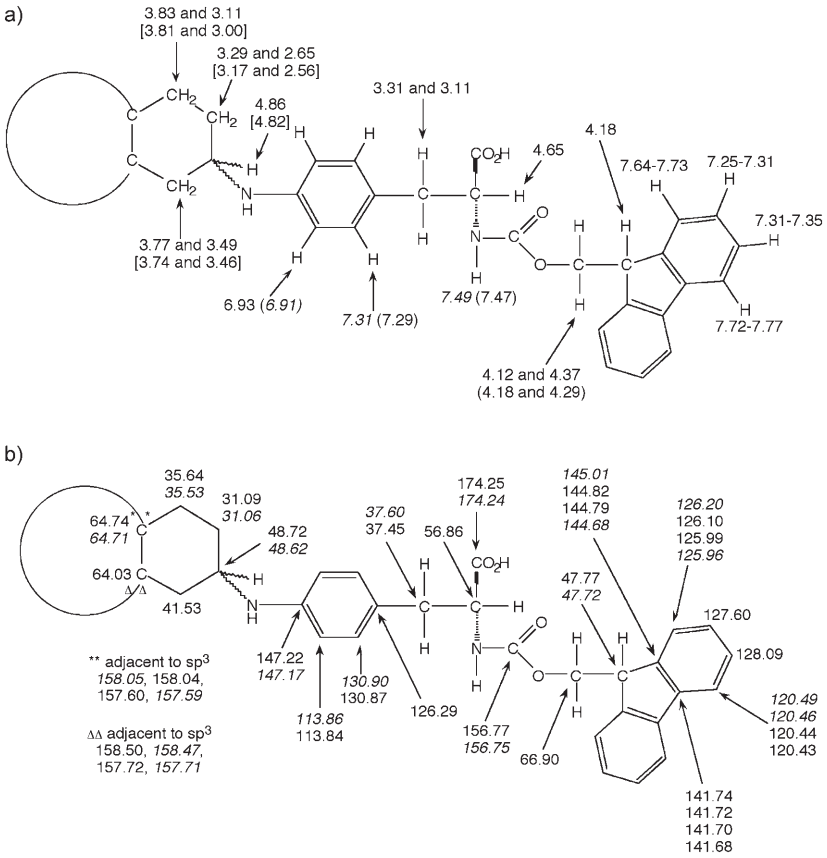

Figure 3. Assignment of (a) ^{1}H and (b) ^{13}C NMR spectra for Fmoc-Baa (**1c**). The stronger ^{13}C signals (presumably from the more abundant diastereomer) when two or four signals are resolved for a given site are in italics. These signals are tentatively assigned to the (*R*,*S*) diastereomer. A few ^{1}H signals can be similarly assigned on the basis of intensity and are also shown in italics. The ^{1}H signals in the six-membered saturated ring of one diastereomer are enclosed in brackets, while the corresponding signals from the other diastereomer are not. In most cases, the pairs of ^{1}H signals for corresponding sites in the rest of the molecule cannot be assigned to specific diastereomers; one of these signals is in parentheses.

amounts of the (*R*,*S*) and (*S*,*S*) diastereomers indicates that hydrogenation of the imine was not sterically influenced. The -NHC(O)CH_3 and -C(O)OCH_3 protecting groups on the amino acid apparently exerted very similar spatial effects during hydrogenation. The absence of symmetry in **1a** makes all 58 fullerene sp^2 carbons inequivalent, which is apparent from the numerous sp^2 carbon signals downfield of $\delta = 135$ ppm in the ^{13}C spectrum. All 58 fullerene sp^2 carbon signals are detected. More than 58 signals appear to be present, consistent with the presence of two diastereomers, in light of the very small splittings or shoulders evident on some signals. Only one of the phenyl carbon signals (from C-N, at $\delta = 147.0123$ ppm) falls within the fullerene sp^2 carbon region. One might conclude just on the basis of ^{13}C chemical shifts that the four rather deshielded fullerene sp^2 signals (from $\delta = 157.29$ to $\delta = 158.22$ ppm) result from the four carbons adjacent to the two fullerene sp^3 sites. This was confirmed by the HMBC experiment, which showed that these four fullerene sp^2 carbons correlated with the protons (via $^{3}J_{C,H}$ and possibly $^{4}J_{C,H}$ couplings) at $\delta = 3.759$, 3.634, 3.397, and 2.990 ppm. It was not possible to assign these four fullerene sp^2 ^{13}C signals to specific carbons adjacent to a fullerene sp^3 site. The two fullerene sp^3 sites were differentiated on the basis that only the signal at $\delta = 63.91$ ppm exhibits a long-range correlation to the methine proton at $\delta = 4.81$ ppm, only the signal at $\delta = 64.55$ ppm exhibits a long-range correlation to the methylene protons at $\delta = 2.55$ and 3.22 ppm, and the expectation that correlations via $^{3}J_{C,H}$ would be stronger than those via $^{4}J_{C,H}$ in an experiment optimized for a long-range $J_{C,H}$ value of 7.0 Hz. In general, the various ^{1}H and ^{13}C signal assignments for Baa (**1a**) follow in a rather straightforward fashion from the 1D and 2D NMR experiments and are consistent with relevant model compound data.[22,23]

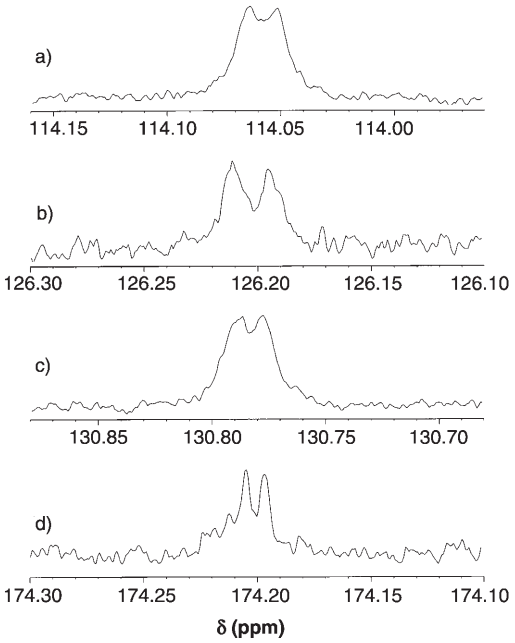

Figure 4. Expanded regions (each only 0.20 ppm wide) of the ^{13}C spectrum of Baa (**1a**) showing pairs of signals of essentially equal intensity for a given site in the two diastereomers: a) the phenylalanine *C*H *ortho* to NH, b) the phenylalanine quaternary *C* next to CH_2, c) the phenylalanine *C*H *ortho* to CH_2, and d) the phenylalanine *C*O_2H.

Converting the NH_2 group in compound **1a** to the NH-Fmoc group in compound **1c** gives a mixture of (*R*,*S*) and (*S*,*S*) diastereomers where many more pairs of signals were resolved in a different mixed-solvent system (1:1 [D_7]DMF:[D_8]toluene). Figure 3 shows the ^1H and ^{13}C NMR assignments for the diastereomeric mixture (*R*,*S*) and (*S*,*S*) of Fmoc-Baa (**1c**). Unlike **1a**, unequal intensities are observed for the pairs of ^{13}C signals from corresponding carbons of the two diastereomers of **1c**, which allows a set of ^{13}C signals to be assigned to one diastereomer and another set of ^{13}C signals to be assigned to the other diastereomer (Figure 5). The presence of the bulky Fmoc group apparently results in one side of the imine being somewhat favored for hydrogenation, which would result in the predominant isomer having (*R*) stereochemistry in the six-membered aliphatic ring. The complex and often overlapping ^1H multiplets usually preclude visual identification of the more intense multiplet for the two diastereomers. However, the relatively simple pair of doublets observed for the carbamate NH in the two diastereomers and for the upfield phenylalanine aromatic H in the two diastereomers allows the stronger doublet in each pair to be tentatively assigned to the (*R*,*S*) diastereomer. The pair of downfield phenylalanine aromatic H doublets in the two diastereomers is obscured in the 1D ^1H spectrum by signals from residual [HD_7]toluene, but from the correlations in the COSY spectrum, it appears that the signal at $\delta = 6.91$ ppm correlates with that at $\delta = 7.31$ ppm and that the signal at $\delta = 6.93$ ppm correlates with that at $\delta = 7.29$ ppm.

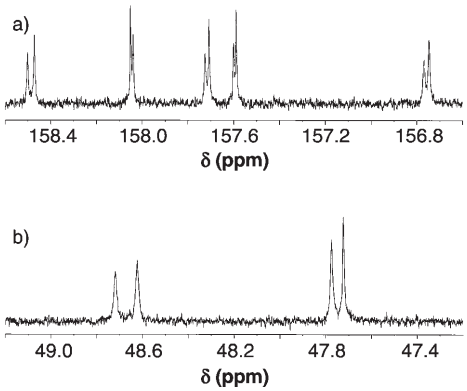

Figure 5. Expanded regions (each only 2.00 ppm wide) of the ^{13}C spectrum of Fmoc-Baa (**1c**) showing pairs of signals differing in intensity for a given site in the two diastereomers. a) The four C_{60} sp^2 carbons in each diastereomer next to an sp^3 carbon ($\delta = 158.502$ to 157.598 ppm) and the carbamate carbon in each diastereomer ($\delta = 156.767$ and 156.746 ppm). b) The aliphatic methine carbon in the six-membered ring ($\delta = 48.718$ and 48.623 ppm) and the Fmoc aliphatic methine carbon ($\delta = 47.775$ and 47.724 ppm).

In the ^1H spectrum, the carbamate NH gives a doublet ($^3J_{HH}$ coupling to the phenylalanine methine proton) for each diastereomer. The doublets are centered at $\delta = 7.495$ and 7.467 ppm and also are the only downfield protons that do not correlate in the ^1H–^{13}C HSQC spectrum. The carbamate NH and phenylalanine methine protons do correlate in the COSY spectrum. The two diastereomers give different carbamate carbonyl signals ($\delta = 156.767$ and 156.746 ppm) that are unambiguously differentiated from the fullerene sp^2 carbon signals through long-range correlations to the phenylalanine methine, carbamate NH, and Fmoc OCH_2 proton signals (see below). Two different ^1H signals appear for the two inequivalent protons in the Fmoc methylene group in the (*R*,*S*) diastereomer, and two more signals appear for the two inequivalent protons in the Fmoc methylene group in the (*S*,*S*) diastereomer. (One AB quartet is at $\delta = 4.37$ and 4.12 ppm; the other AB quartet is at $\delta = 4.29$ and 4.18 ppm.) Because of the chirality of compound **1c**, the two halves of the fluorenyl moiety also are not equivalent, and this sometimes manifests itself through four ^{13}C NMR signals appearing for a pair of fluorenyl sites (Figure 6). For example, two different signals appear for fluorenyl C-1 and fluorenyl C-8 in the (*R*,*S*) diastereomer, and two more signals appear for fluorenyl C-1 and fluorenyl C-8 in the (*S*,*S*) diastereomer: the four signals are at $\delta = 126.197$, 126.104, 125.995, and 125.963 ppm, respectively.

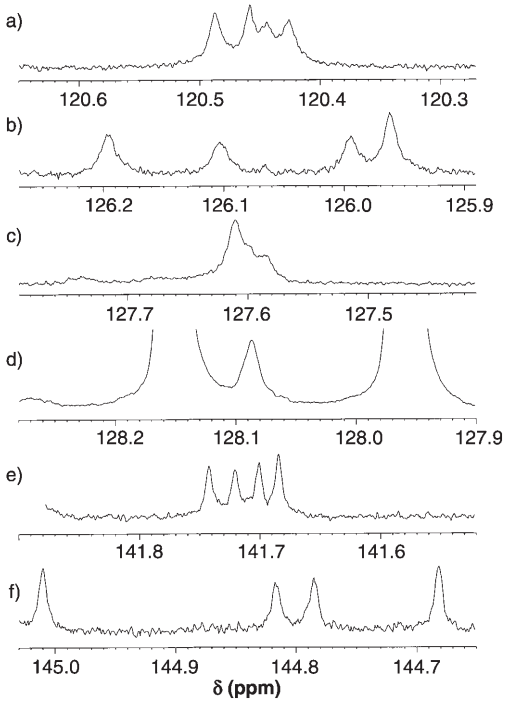

Figure 6. Expanded regions (each only 0.38 ppm wide) of the ^{13}C spectrum of Fmoc-Baa (**1c**) showing the fluorenyl signals for a given site in the two diastereomers. a) The signals for the fluorenyl C-4/C-5 carbons, b) the signals for the fluorenyl C-1/C-8 carbons, c) the highly overlapping signals for the fluorenyl C-2/C-7 carbons, d) the completely overlapped signals for the fluorenyl C-3/C-6 carbons (and intense signals from [D_8]toluene), e) the signals for the fluorenyl C-4a/C-4b carbons, and f) the signals for the fluorenyl C-8a/C-9a carbons.

The 1D and 2D NMR analyses of compound **1c** yield detailed assignments of ^1H and ^{13}C chemical shifts for the two diastereomers, as shown in Figure 3. The COSY experiment

enables the ^{1}H shifts in the saturated six-membered ring of one diastereomer to be differentiated from the ^{1}H shifts in the saturated six-membered ring of the other diastereomer. The inequivalence of the two aromatic rings in the fluorenyl moiety clearly has an effect on the magnetic environment of the protons in the ring adjacent to the fullerene and in the phenylalanine aromatic ring, as ^{1}H signals for each of the diastereomers can clearly be detected (unlike **1a**). Many more pairs of ^{13}C signals are also resolved for sites in **1c** than in **1a**. With a digital resolution less than 0.20 ppm in the ^{13}C dimension of the HSQC and HMBC experiments, many specific assignments can be made. Some of the most critical information obrtained from the HMBC experiment (optimized for $^{1}J_{C,H}=145$ Hz and long-range $J_{C,H}=7.0$ Hz) follows. The carbamate carbonyl signals can clearly be differentiated from the fullerene sp^2 carbon signals, as the pair of ^{13}C signals at $\delta=156.75$ and 156.77 ppm in the 1D experiment exhibits distinctive long-range couplings to the Fmoc CH_2, phenylalanine methine CH, and carbamate NH not observed for the eight fullerene sp^2 ^{13}C signals from $\delta=157.59$ to 158.50 ppm. In addition, these four pairs of fullerene sp^2 ^{13}C signals can be divided into two groups in light of significant differences in their long-range coupling patterns. Only the pair of signals at $\delta=157.59$ and 157.60 ppm and the pair of signals at $\delta=158.04$ and 158.05 ppm exhibit long-range coupling to the protons at $\delta=3.00$ and 3.11 ppm, and thus these four ^{13}C signals can reasonably be assigned as three-bond couplings. Similarly, only the pair of signals at $\delta=$ 157.71 and 157.72 ppm and the pair of signals at $\delta=158.47$ and 158.50 ppm exhibit long-range coupling to the protons at $\delta=3.46$ and 3.49 ppm, and thus these four ^{13}C signals can reasonably be assigned as other three-bond couplings. The first set of four ^{13}C signals also exhibits three-bond couplings to the protons at $\delta=3.81$ and 3.83 ppm, and the second set of four ^{13}C signals also exhibits three-bond couplings to the protons at $\delta=3.74$ and 3.77 ppm.

In the HMBC experiment, the fluorenyl quaternary sp^2 carbon signals can clearly be differentiated from the fullerene sp^2 carbon signals, as only the former exhibit long-range couplings to aromatic protons and to Fmoc aliphatic protons. The four fluorenyl quaternary sp^2 ^{13}C signals from $\delta=$ 145.01–144.68 ppm exhibit much stronger long-range couplings to the Fmoc aliphatic protons than do the four fluorenyl quatenary sp^2 ^{13}C signals from $\delta=141.74$–141.68 ppm, which strongly suggests that the more downfield set of ^{13}C signals results from C-8a and C-9a (two- and three-bond couplings to Fmoc CH and CH_2), while the more upfield set of ^{13}C signals results from C-4a and C-4b (three- and four-bond couplings to Fmoc CH and CH_2). We also believe that the signal at $\delta=145.01$ ppm results from a fluorenyl carbon rather than from a fullerene carbon because the 1D ^{13}C signal at $\delta=145.01$ ppm is similar in linewidth to the signals at $\delta=144.82$, 144.79, and 144.68 ppm but clearly broader than any of the signals just downfield of it.

In the HMBC experiment, the six-membered ring aliphatic methine carbon signals at $\delta=48.72$ and 48.62 ppm can clearly be differentiated from the fluorenyl aliphatic methine carbon signals at $\delta=47.77$ and 47.72 ppm, as the more downfield pair of ^{13}C signals exhibits multiple long-range correlations only to protons upfield of $\delta=4.0$ ppm, while the more upfield pair of ^{13}C signals exhibits multiple long-range correlations only to aliphatic protons downfield of $\delta=$ 4.0 ppm and to fluorenyl aromatic protons. Secure identification of the fluorenyl aliphatic methine carbon signals ($\delta=$ 47.77 and 47.72 ppm) in turn enables the fluorenyl aliphatic methine proton signal to be identified through the HSQC experiment (an assignment reinforced by the distinctive coupling from the Fmoc methylene carbon to the Fmoc methine proton in the HMBC experiment). This methine proton is not readily detected in the 1D ^{1}H spectrum because of the highly second-order nature of the Fmoc CH-CH_2 spin system. In the HMBC experiment, the pair of fullerene quaternary aliphatic signals near $\delta=64.72$ ppm (which couple to the methylene protons at $\delta=2.65$ and 2.56 ppm but not to the methine proton near $\delta=4.85$ ppm) can clearly be differentiated from the unresolved pair of fullerene quaternary aliphatic signals at $\delta=64.03$ ppm (which do not couple to these methylene proton signals but do weakly couple to the methine proton).

Peptide synthesis using fullerene-derivatized amino acids: To date, both solution and solid-phase peptide synthesis (SPPS) methods have been used to prepare fullerene peptides. The preparation of fullerene peptides from SPPS has been shown to have great advantage over solution phase methods, as it greatly simplifies the purification process. However, to incorporate fullerene amino acid into peptide chain using the SPPS is still a challenging task for a couple of reasons: 1) the range of fullerene amino acids that are suitable for SPPS is still limited; 2) fullerene readily aggregates inside hydrophobic network of resins used in SPPS.

The preparation of fullerene peptides from SPPS was first pioneered by Prato and co-workers using Fmoc (9-fluorenylmethoxycarbonyl protected) chemistry with great potential as therapeutic candidates.[24] The classical deprotection agent for Fmoc protecting group is piperidine. Prato and co-workers initially reported that they could achieve the deprotection with piperidine. However, their subsequent work suggested this result was erroneous as piperidine forms multiple stable adducts with the fullerene core! To overcome this problem, these researchers suggested the use of 5% DBU in DMF under a N_2 atmosphere. We have applied the same method; however, we experienced great difficulty in obtaining a pure product even after HPLC purification. The broadness of the HPLC chromatogram leads us to suspect that either DBU or the intermediate coming from the deprotection of Fmoc may also form adducts with the fullerene. A recent publication by Watanabe et al. confirmed our suspicion.[25] Although it is believed that DBU forms only a *mono*-Zwitterionic complex, they showed that it is very capable of interfering with mass spectrometry measurement and HPLC purification. These difficulties in purification led us to develop N-Boc chemistry for Baa-peptides.

As a first step in demonstrating the suitability of the Baa derivatives for SPPS, we have previously reported that the coupling of N-Boc-Baa with the ethoxy ester-protected glycine (NH_2-Gly-OEt) may be carried out in 4:1 DCM/DMF in the presence of HBTU and NEt_3.[14] The parent ion of the final coupling product was observed by MALDI-MS (*m*/*z* 1141), while the peak associated with N-Boc-Baa (*m*/*z* 1056) was completely gone, indicating a high yield reaction. A similar reaction occurs for Fmoc-Baa (**1c**) to give the coupled product **12** (Scheme 2 and Experimental Section).

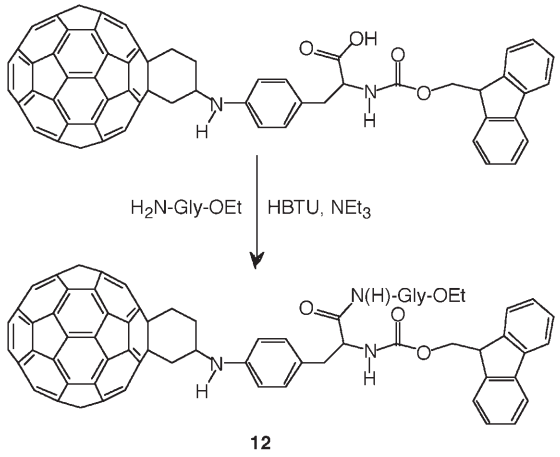

12

Scheme 2. Coupling reaction of Fmoc-Baa (**1c**) with ethoxy ester-protected glycine.

These results clearly demonstrate excellent reactivity of fullerene amino acids and their potential as building blocks in solid-phase peptide synthesis to make fullerene peptides.

The choice of peptide sequences to be investigated in the present study was defined by the application to which they were to be aimed and the desire to make peptide sequences with a range of charges and lengths. Cationic Baa-$(Lys)_9$-OH (**13**) and Baa-Lys(FITC)-$(Lys)_8$-OH (**14**, where FITC = fluorescein isothiocyanate), anionic Baa-$(Glu)_4$-$(Gly)_3$-Ser-OH (**15**), and Baa-$(Glu)_4$-$(Gly)_3$-Ser-Cys-OH (**16**) peptide sequences have been prepared. The anionic peptide **15** was also compared to the parent amino acid for antioxidant activity. In addition, the presence of the cysteine's sulfur also allows SAMs of peptide **16** to be grown on gold surfaces. The Baa derivative of the cell penetrating peptide, Penetratin, has also been prepared (**17**).

To study how the presence and position within the peptide sequence of the fullerene affects the structure and relative structural stability of the peptide's conformation, we used the heptad (HP) sequences Glu-Ile-Ala-Gln-Leu-Glu-Tyr-Glu-Ile-Ser-Gln-Leu-Glu-Gln-NH_2 (2HP) and Glu-Ile-Ala-Gln-Leu-Glu-Tyr-Glu-Ile-Ser-Gln-Leu-Glu-Gln-Glu-Ile-Gln-Ala-Leu-Glu-Ser-NH_2 (3HP) due to the well-understood secondary structure, structural interconversions, and self-assembly processes.[26] Key locations will involve replacing tyrosine (Tyr) with Baa in 2HP (i.e., Glu-Ile-Ala-Gln-Leu-Glu-Baa-Glu-Ile-Ser-Gln-Leu-Glu-Gln-NH_2, **18**) and the addition of Baa to the C-terminus, i.e., Baa-2HP (Baa-Glu-Ile-Ala-Gln-Leu-Glu-Tyr-Glu-Ile-Ser-Gln-Leu-Glu-Gln-NH_2, **19**) and Baa-3HP (Baa-Glu-Ile-Ala-Gln-Leu-Glu-Tyr-Glu-Ile-Ser-Gln-Leu-Glu-Gln-Glu-Ile-Gln-Ala-Leu-Glu-Ser-NH_2, **20**).

For each of the peptides the appropriate sequence was first synthesized on an automated peptide synthesizer using standard 9-fluorenylmethoxycarbonyl (Fmoc) chemistry (see Experimental Section). The coupling between N-Boc-Baa and the appropriate sequence was performed manually by using PyBOP/HOBt/DiEA (PyBOP = 1*H*-benzotriazol-1-yloxytripyrrolidino-phosphonium hexafluorophosphate, HOBt = *N*-hydroxybenzotriazole, DiEA = diisopropylethylamine) in a three-fold excess. For peptide **14** the fluorescent marker was introduced by selective removal of the Mtt protecting group using 1% trifluoroacetic acid (TFA) in CH_2Cl_2 with 5% triisopropylsilane (TIPS) followed by reaction with fluorescein isothiocyanate (FITC). The final peptide was cleaved from resin by concentrated TFA/TIPS/H_2O (95:2.5:2.5) cocktail with concurrent deprotection of all amino acid side chains. The peptide solutions were concentrated at room temperature and precipitated and washed with cold Et_2O. The final purification was achieved by semi-preparative Luna C5 and preparative Dynamax C18 columns for Baa-containing and parent peptides, respectively. HPLC analysis, using a 0.1% TFA in H_2O/IPA gradient (see Experimental Section), showed one major product for all peptides. This is in contrast with our efforts using the Fmoc protection methodology. Furthermore, the high yield of the Baa-terminated peptides appears to be independent of the length of the peptide. However, the yield of the fullerene peptide does show a dependence on the hydrophobicity of the peptide sequence: the more hydrophilic the sequence, the higher the yield.

For all the fullero-peptides (**12**–**20**) the isolation of the desired sequence is confirmed by the presence of the M^+ or $M^+ + H$ ion in the MALDI-TOF mass spectrometry. For some of the sequences the observation of the parent ion $[M^+]$ is accompanied with peaks due to the addition of Group 1 metals, for example, $[M^+ + Na]$ or $[M^+ + Na + K]$. The majority of the Baa-functionalized peptides are sufficiently soluble in H_2O to provide a UV/Vis spectrum. The observed spectra are consistent with absorption of C_{60}, and the amide region of the peptide (Figure 7).

We have previously observed that the parent amino acid, Baa, aggregates in aqueous solution,[15] presumably as a consequence of the presence of both hydrophobic and hydrophilic groups within the same molecule. It is reasonable to suppose that the peptides that are soluble in water would also form aggregates. The particle size in solution was determined by dynamic light scattering (DLS) for Baa-peptides, **13** and **14**. Solutions in the range of 0.125–2.0 mg mL^{-1} were prepared using PBS buffer prepared from HPLC grade water and were filtered through a 0.10 mm cup filter (Millipore, Express). The solution aggregation of **14** was compared with its non-FITC containing analogue (**13**) to determine the effects of the FITC. The peptides all show aggrega-

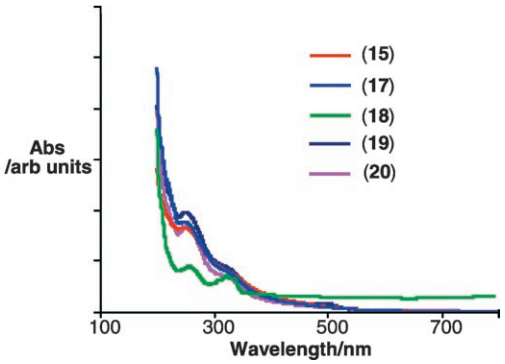

Figure 7. UV/Vis spectrum of fullerene peptides in aqueous solution.

tion in aqueous solution across the concentration ranges measured. The poly-lysine peptide **13** exhibits a single broad aggregate distribution (50–350 nm) with an average size of about 200 nm. The size of the aggregate is independent of concentration (0.25–2.0 mg mL^{-1}), although the distribution narrows with increased concentration. In contrast, FITC-labeled poly-lysine peptide **14** shows two distinct aggregate sizes at concentrations between 0.125 and 1.0 mg mL^{-1}. The major component (ca. 60%) is comparable in size (ca. 180 nm) to that seen for **14**. The minor component is a smaller aggregate (ca. 10 nm) with a relatively narrow distribution (5–20 nm). At high concentrations (2.0 mg mL^{-1}) a third larger aggregate (ca. 1500 nm) is observed at the expense of both of the other aggregate sizes (see Figure 8).

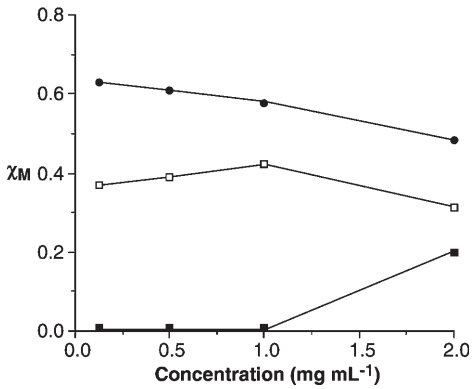

Figure 8. Plot of the fraction of aggregates for Baa-Lys(FITC)-Lys$_8$-OH (**14**) as a function of solution concentration. Average aggregate size = 10 nm (□), 180 nm (●), and 1500 nm (■).

To further examine the actual aggregate size and morphology, cryo-TEM experiments were performed for peptide **14**. The result showed that fullerene peptides exhibited strong aggregation behavior in aqueous solution, a similar phenomenon demonstrated by other water-soluble fullerene derivatives.[27] The peptide forms spherical and ellipsoidal clusters, with an average aggregate size of 40–80 nm, which are generally smaller than the diameters observed by DLS. There are two dominant groups in size (Figure 9); one type has the diameter of 40–80 nm with predominant population

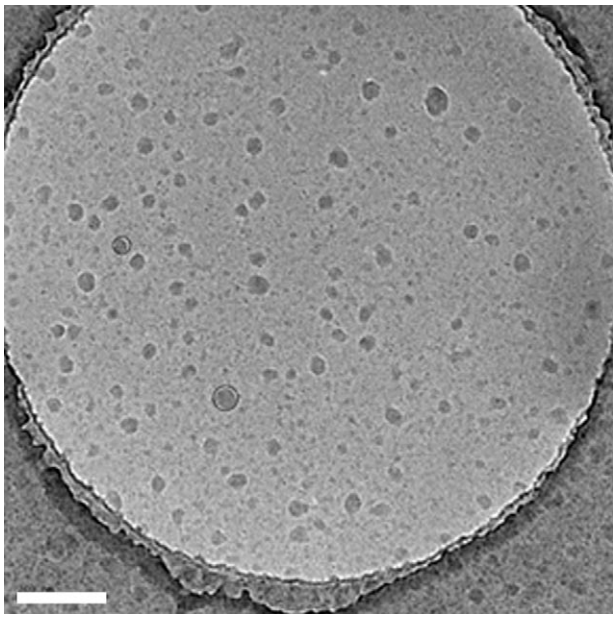

Figure 9. Vitreous ice cryo-TEM image of the aggregates formed by Baa-Lys(FITC)-Lys$_8$-OH (**14**) in PBS buffer (1 mg mL^{-1} @ pH 7). Scale bar = 200 nm.

at a size of about 50 nm, and the other population has a diameter less than 20 nm, which may correspond to the size of fullerene peptides itself.

The presence of the FITC residue does have a dramatic affect on the self-assembly of the fullerene–peptide nanostructures. Georgakilas et al. have demonstrated that the addition of a large planar π-ligand (porphyrin) to a fullerene derivative containing a short organic side chain terminated by an ionic residue changes the ordering from a 4-nm diameter nanorod of variable length to uniform nanotubules with a diameter of 30 nm and length of 500 nm.[28] It is proposed that this change is associated with either porphyrin–porphyrin or C_{60}–porphyrin interactions that are larger than the C_{60}–C_{60} interactions. Given that the FITC residue may have a comparable effect between peptides **13** and **14**, incorporation of peptides **13** and **14** into 10% SDS in PBS buffer allowed for imaging any aggregates by TEM. Baa-(Lys)$_9$-OH (**13**) shows unpatterned aggregates network. In contrast, the TEM images of Baa-Lys(FITC)-(Lys)$_8$-OH (**14**) show the formation of large fibers (Figure 10). Each fiber appears to be a nano-tubule with a diameter of 100 nm and length over 5 μm. Furthermore the nano-tubules form aligned bundles. The presence of the FITC ligand has a significant impact on the aggregation and self-assembly of the Baa-containing peptides. It should be noted that these results might have implications for the cellular uptake of the peptides as SDS can be viewed as the simplest form of cell membrane.

The circular dichroism (CD) spectra of the Baa-substituted peptides (**18**–**20**) were compared to those of the native peptides to determine the effect on the secondary structure. The parent 2HP adopts a random coil configuration above pH 7. As the pH is lowered, it exhibits a α-helix structure as a transition to the formation of β-sheets below pH 7. The

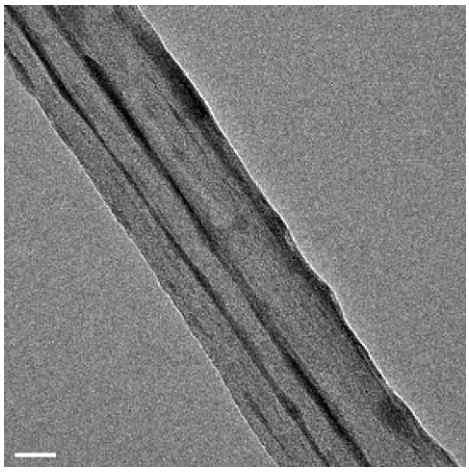

Figure 10. TEM images of Baa-Lys(FITC)-Lys_8-OH (**14**) with 10% SDS in PBS buffer. Scale bar = 50 nm.

addition of the Baa, irrespective of the position, has a dramatic effect on the relative stability of the peptide secondary structure as compared to 2HP; however, the position of substitution alters the mode of the effect (Table 2). Positioning the Baa in the center of the 2HP sequence by replacement of tyrosine (i.e., **18**) resulted in a circular dichroism (CD) consistent with the formation of a β-sheet structure across the pH range 3–11. Thus, the presence of the C_{60} has a clear stabilization effect on the stability of the β-sheet conformation. We note that the CD does not exclude the presence of other conformations, but indicates the β-sheet is the major conformation. The conversion from β-sheet to α-helix may be induced by the addition of CF_3CH_2OH.

Table 2. Structural transformations as a function of pH for fullerene-peptides.

Peptide	Secondary structure with decreasing pH	Appearance
2HP	random coil → α-helix → β-sheet	fibers
18	β-sheet	fibers[a]
19	random coil → α-helix	aggregates
3HP	random coil → α-helix	fibers
20	α-helix	coiled fibers

[a] TEM images show areas with aggregated structure.

In contrast to the results for substitution in the center of the peptide, addition of Baa to the C-terminus of 2HP results in a peptide (Baa-2HP, **19**) whose CD indicates the formation of a weak random coil under basic conditions, that is, in a similar manner to the parent 2HP. Upon reduction of the solution pH, the structure of **19** transforms to a α-helix; however, unlike 2HP, peptide **19** does not subsequently convert to a β-sheet conformation (Table 2). Instead, slow precipitation of an aggregate occurs at pH 6 with more rapid precipitation of the same material occurring at lower pH.

The solution conformation of 3HP at high pH is that of a random coil; however, with decreasing pH an α-helix is formed (Table 2) that results in the formation of a short fiber-like structure: upon aging longer fibers are formed. In contrast, the C-terminus Baa-functionalized 3HP (Baa-3HP) shows the formation of a weak α-helix structure even at high pH.

Antioxidant properties: The antioxidant assay of Baa was determined in DMSO/PBS buffer (1:1). As may be seen from Figure 11, the parent amino acid is a very potent antioxidant with an IC_{50} of 55.88 μM through an established method.[29] This is about 10 times more potent than Trolox, a commercially available potent antioxidant of the vitamin E family (**II**). The antioxidant study demonstrated a linear relation for the inhibition versus concentration of the fullerene amino acid and is consistent with the electrochemical behavior of fullerene amino acids showing the ability of the fullerene core to accept multiple electrons (see above).

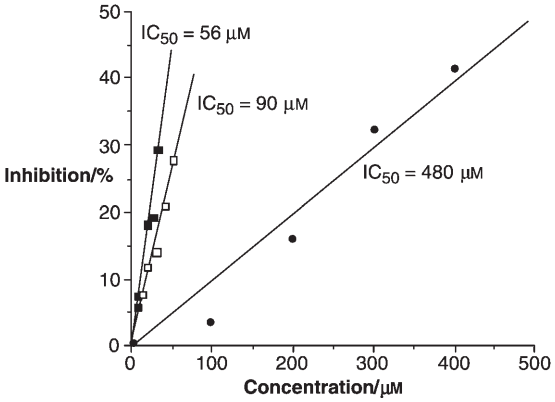

Figure 11. Plot of inhibition (%) as a function of reagent concentration for antioxidant activity comparison using Baa (■), peptide **15** (□), and Trolox (●).

Given the above result and the facile ability of Baa-derived peptides to transport into a cell, we are interested if a Baa-containing peptide retains the antioxidant properties of the Baa residue. Furthermore, if the peptide shows anti-oxidant properties, is it comparable with regard to the C_{60} content? The IC_{50} of Baa-$(Glu)_4$-$(Gly)_3$-Ser-OH (**15**) was determined to be 89 μM. A plot of inhibition as a function of concentration for peptide **15** is shown in Figure 11. Based upon this assay it is apparent that while the anionic peptide **15** has about five fold the activity of Trolox (IC_{50} = 480 μM), its molar activity is not as good as Baa itself (IC_{50} = 55 μM). It is unclear at the present for the reason for the slight reduction in activity between Baa and the Baa-containing peptide **15**. It is possible that aggregation of the Baa-peptide results in the "$(Glu)_4$-$(Gly)_3$-Ser-OH" being exposed to the solution, and acting as a buffer limiting electron transfer processes. Further studies will be necessary to fully understand the effectiveness of the Baa-peptides; however, the ability of Baa-derived peptides to transport into a cell and show antioxidant properties is worthy of further study. Fullerene peptides with cationic sequences show no antioxidant activity.

C_{70}-Derived amino acids: Although C_{60}-derived amino acids are well documented in the literature, there are no examples of amino acids derived from C_{70}. Given the flexibility of our methodology for C_{60}-derived amino acids, we have extended this approach to the synthesis of the first C_{70}-derived amino acids.

Following the same Diels–Alder reaction used for C_{60}, the ketone precursor (**21**)[30,31] is readily prepared by the reaction of 2-trimethylsilyloxy-1,3-butadiene with C_{70}. The N-Boc-protected C_{70} phenylalanine derivative (**22**) is obtained in good yield by the reaction of the C_{70}-ketone (**21**) and N-Boc-protected 4-aminophenylalanine; C_{70}-phenylalanine (**23**) can be produced in good yield (see Experimental Section).

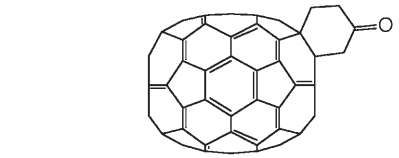

21

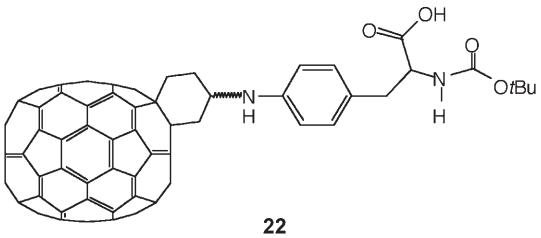

22

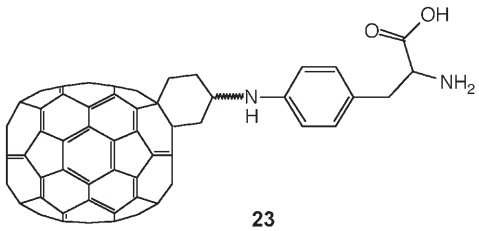

23

For simplicity, just one possible addition product of 2-trimethylsilyloxy-1,3-butadiene to C_{70} has been shown (**21**). The lack of symmetry in 2-trimethylsilyloxy-1,3-butadiene allows addition to occur to give the other regioisomer. The lower symmetry of C_{70} (D_{5h}) also allows for addition to occur at other bonds. Thus, multiple different ketones can in principle form, each of which would give two diastereomers upon hydrogenation of the imine to generate the amine. Detailed NMR analysis[32] indicates that a mixture of three ketones in a 4:1:2 ratio is initially formed and subsequently converted to a mixture of the corresponding six amines. The three ketones result from the two regioisomers generated upon addition to the C_{70} *a*–*b* bond (the most abundant isomer being **21** and the least abundant isomer being the other regioisomeric ketone) and from the single isomer generated upon addition to the C_{70} *c*–*c* bond. Of the six amines, one diastereomer clearly predominates. Its structure and ^{1}H and ^{13}C shift assignments are shown in Figure 12. We are continuing our studies of the C_{70}-derivatives to ascertain differences in cell uptake and toxicology.

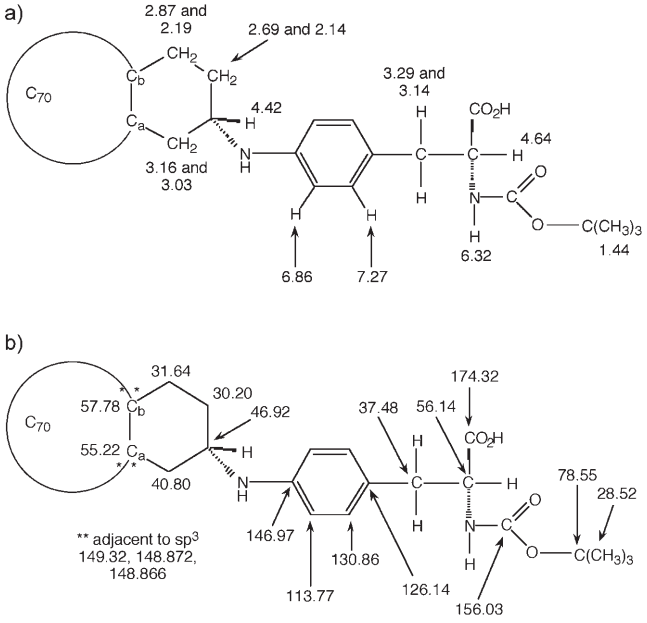

Figure 12. Assignment of a) ^{1}H and b) ^{13}C NMR spectra for the major diastereomer of N-Boc-C_{70}-Phe-OH (**22**). In addition to the known stereochemistry of the amino acid moiety, the deduced stereochemistry of the aliphatic six-membered ring and the deduced *a* and *b* site assignments for the sites of addition to C_{70} are shown.

Conclusions

In summary, we report that a new route to fullerene-based phenylalanine has been established through the condensation reaction of 1,2-(4′-oxocyclohexano)fullerene with amines to form imine intermediates followed by the selective reduction of the imine. This synthetic methodology is extended to lysine derivatives as well as bifunctional derivatives of [60]fullerene (C_{60}). A common property of the fullerene amino acids prepared herein is their stability to hydrolytic and enzymatic cleavage. Electrochemical studies showed that the fullerene core is intact. The as produced [60]fullerene phenylalanine derivatives have shown excellent antioxidant activity. We have shown that we can synthesize fullerene peptides in relatively large scale via solid phase peptide synthesis. Based upon our results it appears that the yield of the fullerene peptide is dependent on the hydrophobicity of the peptide sequence.

Experimental Section

All reactions were performed under an atmosphere of nitrogen or argon unless stated otherwise. Fullerene (>99.5% pure) was purchased from

MER and used as received. All solvents were dried before use. Toluene was distilled over sodium. THF was distilled over Na/benzophenone. Ethyl acetate was distilled over CaH_2. Flash column chromatography was performed using 230–400 mesh silica gel from EM Science. Rink amide and Wang resin were obtained from Novabiochem, USA. Amino acids were purchased from Novabiochem and used as received. MALDI-TOF mass analysis was performed on a linear Protein-TOF Bruker BinFlex-III MALDI instrument using sulfur as the matrix. UV/Vis spectra were recorded on a Varian Cary 5000 spectrometer. DLS Measurements were performed on the samples using a Brookhaven 90Plus submicron particle-size analyzer with HeNe laser (30 mW) that operates at 656 nm wavelength. Solutions were made in PBS buffer prepared from HPLC grade water, and filtered through a 0.10 mm cup filter (Millipore, Express). TEM measurements were performed on a JEOL 2010 TEM at 200 kV. Images were taken in the concentration of 1.0 mg mL^{-1} and samples were prepared by dipping a copper grid coated with amorphous lacy carbon grid into the sample solution. The images were mainly taken in the "hole" region of the grid to minimize the artificial effect from the samples or ice.

NMR spectroscopy: ^{1}H and ^{13}C NMR spectra were recorded on Bruker Avance-400 and 500 spectrometers. 2D-NMR experiments (^{1}H–^{1}H COSY, ^{1}H–^{13}C HSQC, and ^{1}H–^{13}C HMBC) were performed on a Bruker 500 spectrometer. Samples were dissolved in the indicated solvent system. For each sample, a vortex plug was used to minimize solvent evaporation during the NMR experiments on the 500 MHz spectrometer. A general description of the NMR probes and methodology used has been previously reported.[33]

*Baa (**1a**)*: Mixed solvent of [D_8]toluene, [D_4]methanol, and [D_6]DMSO. ^{1}H: 90° pulse, 5.03 s FID, 5 s relaxation delay, 32 scans, no line broadening used in processing FID zero-filled from 64 K to 128 K. ^{13}C: 90° pulse, 5.23 s FID, 5 s relaxation delay, 5,728 scans, 0.2 Hz line broadening used in processing 256 K FID. DEPT-135 ^{13}C optimized for $J_{C,H}=145$ Hz, 2.61 s FID, 5 s relaxation delay, 2080 scans, 0.5 Hz line broadening used in processing 128 K FID. COSY: 256 increments, 4 scans/increment. HSQC optimized for $^1J_{C,H}=145$ Hz; 256 increments, 72 scans/increment. HMBC optimized for $^1J_{C,H}=145$ Hz and long-range $J_{C,H}=7.0$ Hz; 256 increments, 336 scans/increment.

*Fmoc-Baa (**1c**)*: 1:1 [D_8]toluene/[D_7]DMF. NMR parameters as for Baa (**1a**) except as follows: ^{1}H: 30° pulse, 6.55 s FID, 10 s relaxation delay, 64 scans, no line broadening used in processing FID zero-filled from 64 K to 128 K. ^{13}C: 90° pulse, 5.61 s FID, 5 s relaxation delay, 6,400 scans, 0.1 Hz line broadening used in processing 256 K FID. DEPT-135 ^{13}C optimized for $J_{C,H}=145$ Hz, 5.61 s FID, 5 s relaxation delay, 1088 scans, 0.1 Hz line broadening used in processing 256 K FID. HSQC 1024 increments (^{13}C digital resolution = 0.17 ppm), 24 scans/increment. HMBC 1024 increments (^{13}C digital resolution = 0.18 ppm), 32 scans/increment.

*N-Boc-C_{70}-Phe-OH (**22**)*: 2:1 [D_8]toluene/[D_7]DMF. NMR parameters as for Baa (**1a**) except as follows: ^{1}H: 30° pulse, 5.45 s FID, 5 s relaxation delay, 280 scans, no line broadening used in processing FID zero-filled from 64 K to 128 K. ^{13}C: 90° pulse, 2.65 s FID, 5 s relaxation delay, 18,600 scans, 0.2 Hz line broadening used in processing FID zero-filled from 128 K to 256 K. DEPT-135 ^{13}C optimized for $J_{CH}=145$ Hz, 2.65 s FID, 5 s relaxation delay, 33,600 scans, 0.2 Hz line broadening used in processing 128 K FID. COSY 1024 increments (F1 digital resolution = 0.0098 ppm), 16 scans/increment. HSQC 1024 increments (^{13}C digital resolution = 0.17 ppm), 24 scans/increment. HMBC 512 increments (^{13}C digital resolution = 0.37 ppm), 224 scans/increment.

N-Ac-C_{60}-Phe-OMe (N-Ac-Baa-OMe): Prepared as previously reported.[14] Yield: 43 %. ^{1}H NMR (400 MHz, [D_8]toluene/[D_4]methanol): $\delta=$ 8.07 (dd, J(H,H) = 2.5, 7.8 Hz, 1H; -NHCOCH$_3$), 7.24 (d, J(H,H) = 8.4 Hz, 2H), 6.92 (d, J(H,H) = 8.4 Hz, 2H), 5.78 (d, J(H,H) = 7.6 Hz, 1H; -NH), 4.93, (dt, J(H,H) = 5.9, 7.8 Hz, 1H; -CH(CO$_2$Me)), 4.80 (m, 1H; -CH (hexagonal ring)), 3.74 (dt, J(H,H) = 4.2, 13.2 Hz, 1H; -CH$_2$(CH$_2$)-(C_{60})), 3.65 (dd, J(H,H) = 10.9, 13.2 Hz, 1H; -CH$_2$(CH)(C_{60})), 3.48 (s, 3H; COOCH$_3$), 3.39 (m, 2H), 3.16 (dd, J(H,H) = 5.8, 13.9 Hz, 1H), 3.04 (dd, J(H,H) = 8.3, 13.7 Hz, 1H; CH$_2$), 2.95 (m, 1H; -CH$_2$ (hexagonal ring)), 2.56 (m, 1H), 1.93 ppm (d, 3H, J(H,H) = 2.8 Hz; COCH$_3$); ^{13}C{^{1}H} NMR: $\delta=$ 173.33 (173.35) 169.80, 158.19, 157.73, 157.36, 157.23, 146.69, 146.51, 146.27, 145.75, 145.74, 145.69, 145.66, 145.64, 142.85, 142.83, 142.44, 142.37, 142.36, 142.33, 141.93, 141.89, 140.62, 140.60, 140.59, 140.48, 136.47, 136.23, 135.31, 135.09, 130.74, 130.73, 113.99, 64.52, 63.84, 54.85 (54.84), 51.70, 48.58, 41.53, 37.71, 35.56, 31.07, 22.92 ppm; UV/Vis: λ_{max} (CH_2Cl_2) = 254, 301, 427, 700 nm; MALDI-TOF MS: calculated for $C_{76}H_{22}N_2O_3$ [M^+], 1010.2, found 1010.6, 880.5.

C_{60}-Phe-OH (Baa, 1a): Prepared as previously reported.[14] ^{1}H NMR (500 MHz, [D_8]toluene/[D_4]methanol) Assignments given in Figure 2a: $\delta=$ 7.255 (d, J(H,H) = 8.4 Hz, 2H), 6.905 (d, J(H,H) = 8.4 Hz, 2H), 4.828 (dd, J(H,H) = 5.2, 8.6 Hz, 1H), 4.81 (m, 1H), 3.759 (ddd, J(H,H) = 4.2, 13.4, 13.4 Hz, 1H), 3.634 (ddd, J(H,H) = 0.7, 10.9, 13.2 Hz, 1H), 3.397 (ddd, J(H,H) = 0.7, 4.9, 13.2, 1H), 3.244 (dd, J(H,H) = 5.2, 14.1 Hz, 1H), 3.22 (m, 1H), 3.036 (dd, J(H,H) = 8.6, 14.1 Hz, 1H), 2.99 (dddd, J(H,H) = 1.0, 4.1, 4.1, 13.4 Hz, 1H), 2.549 ppm (m, 2H); ^{13}C{^{1}H} NMR (125.8 MHz, [D_8]toluene/[D_4]methanol), with values for corresponding carbons in the two diastereomers given in parentheses. More detailed assignments given in Figure 2b: $\delta=$ (174.2054 and 174.1971 Phe COOH), 158.2248 (C_{60} sp^2 next to sp^3), 157.8049 (C_{60} sp^2 next to sp^3), 157.3752 (C_{60} sp^2 next to sp^3), 157.2917 (C_{60} sp^2 next to sp^3), 147.9448, 147.9319, 147.0123 (Phe quaternary next to NH), 146.7596, 146.7533, 146.7069, 146.6950, 146.5504, 146.5266, 146.5112, 146.3082, 146.2888, 146.2000, 146.1665, 146.1380, 146.0390, 146.0273, 145.7697, 145.7552, 145.7067, 145.6880, 145.6800, 145.6587, 145.6454, 145.0986, 145.0927, 145.0536, 145.0154, 143.5295, 143.5056, 142.8650, 142.8479, 142.8271, 142.5380, 142.5085, 142.4556, 142.4282, 142.4240, 142.3893, 142.3624, 142.3539, 142.3411, 141.9530, 141.9277, 141.9218, 141.9118, 141.9045, 141.8988, 140.6067, 140.5862, 140.4902, 136.4672, 136.2479, 135.2900, 135.1312, (130.7871 and 130.7780 Phe CH *ortho* to CH$_2$), (126.2116 and 126.1958 Phe quaternary next to CH$_2$), (114.0640 and 114.0519 Phe CH *ortho* to NH), 64.5506 (C_{60}, sp^3), 63.9063 (C_{60}, sp^3), 54.8348 (Phe CH), (48.6137 and 48.6001 methine in six-membered ring), 41.4371 (CH$_2$), 37.3042 (Phe CH$_2$), 35.5501 (CH$_2$), 30.9998 ppm (CH$_2$); UV/Vis: λ_{max} (H_2O) = 247, 338, 470, 707 nm; MALDI-TOF MS calculated for $C_{73}H_{18}N_2O_2$ [M^+], 954.1, found 950.9, 879.9.

N-Boc-C_{60}-Phe-OH (N-Boc-Baa, 1b): Prepared as previously reported.[14] Yield: 53 %. Select data: ^{1}H NMR (400 MHz, [D_8]toluene/[D_4]methanol): $\delta=$ 7.18 (d, J(H,H) = 8.3 Hz, 2H), 6.73 (d, J(H,H) = 8.3 Hz, 2H), 5.66 (d, J(H,H) = 8.3 Hz, 1H), 4.71 (m, 2H), 3.57 (dd, J(H,H) = 3.5, 13.6 Hz, 1H), 3.41 ≈ 3.03 (m, 5H), 2.92 (m, 1H), 2.38 (m, 1H), 1.41 ppm (s, 9H; OC-(C*H*$_3$)$_3$); UV/Vis: λ_{max} (CH_2Cl_2) = 254, 300, 427, 700 nm; MALDI-TOF MS calculated for $C_{78}H_{26}N_2O_4$ [M^+], 1054.2, found 1054.9, 880.8.

Fmoc-C_{60}-Phe-OH (Fmoc-Baa, 1c): Bucky ketone (316 mg, 0.4 mmol) and Fmoc-Phe(4-NH$_2$)-OH (412 mg, 0.6 mmol) and a catalytic amount of *p*-benzosulfonic acid were added into a 250-mL Schlenk flask equipped with a magnetic stir bar. The starting mixture was pumped dry under vacuum. Then degassed, freshly distilled toluene (300 mL) and dry ethyl acetate (100 mL) were charged into the flask under argon atmosphere. The flask was headed on a Soxhlet extractor filled with oven dried 4 Å molecular sieves. The reaction mixture was refluxed for two days. In a second 250-mL flask, phthalic acid (100 mg) was added and dried with a heat gun in vacuum. The dried phthalic acid was then dissolved in dry THF (15 mL) under argon. After the fullerene imine solution cooled down, the dark golden brown solution was filtered by a cannula to the second Schlenk flask equipped with a magnetic stir bar. The resulting buckyimine solution was then cooled down to −42 °C with a MeCN/dry ice bath. Then, an excess amount BH_3–THF solution (3 mL, 1 M) was injected by syringe. The reaction was completed after 2 h as shown by TLC plate. Then MeOH (2 mL) was injected to quench excess BH_3. The final solution was first washed with dilute $KHCO_3$ solution to carefully adjust the pH to 7 first, then with dilute HCl to remove unreacted Fmoc-Phe(4-NH$_2$)-OH and phthalic acid. The organic phase was dried over Na_2SO_4, and the resulting solution was concentrated on rotorvap and chromatographed on dry silica gel. Next, 195 mg (41 %) of the final product was eluted by toluene/ethyl acetate/acetic acid (100:8:1). Select data: ^{1}H NMR (500 MHz, [D_8]toluene/[D_7]DMF): see Figure 3. ^{13}C{^{1}H} NMR (125.8 MHz, [D_8]toluene/[D_7]DMF), with values for corresponding carbons for the two diastereomers shown with the stronger signal in italics: $\delta=$ (174.2514 and *174.2394* Phe COOH), (158.5019 and *158.4714* C_{60} sp^2

next to sp^3), (*158.0493* and 158.0386 C_{60} sp^2 next to sp^3), (157.7239 and *157.7067* C_{60} sp^2 next to sp^3), (157.6000 and *157.5883* C_{60} sp^2 next to sp^3), (156.7673 and *156.7456* carbamate carbonyl), 147.9638, 147.9344, (147.2253 and *147.1725* Phe quaternary next to NH), 146.7653, 146.7577, 146.7440, 146.7394, 146.6897, 146.6799, 146.5492, 146.5207, 146.5134, 146.4337, 146.3660, 146.3410, 146.3351, 146.2675, 146.2423, 146.1321, 146.1223, 145.7605, 145.7481, 145.7407, 145.7119, 145.6891, 145.6581, 145.6519, 145.6418, 145.6072, 145.6012, 145.1302, 145.1177, 145.1000, 145.0625, 145.0498, 145.0449, (*145.0102*, 144.8177, 144.7856, and *144.6820* fluorenyl C-8a and C-9a), 143.5356, 143.5215, 143.4955, 143.4883, 142.8381, 142.8246, 142.8006, 142.5387, 142.5223, 142.5093, 142.4968, 142.4525, 142.4061, 142.3996, 142.3826, 142.3606, 142.3552, 141.9379, 141.9090, 141.8919, (141.7427, 141.7212, 141.7010, and 141.6849 fluorenyl C-4a and C-4b), 140.5843, 140.5775, 140.5584, 140.5392, 140.4451, 140.4351, 138.0584, 136.5902, 136.5607, 136.3231, 136.2895, 135.4868, 135.4361, 135.2919, 135.2337, (*130.9005* and 130.8734 Phe CH ortho to CH_2), 128.0874 (fluorenyl C-3 and C-6), 127.6108 (fluorenyl C-2 and C-7), 126.2934 (Phe quaternary next to CH_2), (*126.1974*, 126.1038, 125.9948, and *125.9629* fluorenyl C-1 and C-8), (*120.4879*, *120.4586*, 120.4447, and 120.4262 fluorenyl C-4 and C-5), (*113.86* and 113.84 Phe CH ortho to NH), 66.9010 (Fmoc OCH_2), (64.7355 and *64.7144* C_{60}, sp^3), 64.0277 (C_{60}, sp^3), 56.8600 ppm (Phe CH), (48.7179 and *48.6227* methine in 6-membered ring), (47.7753 and *47.7237* Fmoc CH), 41.5286 (CH_2), (*37.5965* and 37.4505 Phe CH_2), (35.6420 and *35.5347* CH_2), (31.0864 and *31.0621* CH_2); UV/Vis: λ_{max} (CH_2Cl_2) = 256, 296, 322, 431 nm; MALDI-TOF MS calculated for $C_{88}H_{28}N_2O_4$ [M^+], 1176.2, found 1176.2, 880.3.

N-Ac-C_{60}-Lys-OMe (2): Bucky ketone (136 mg, 0.18 mmol), Ac-Lys(4-NH_2)-OMe (95 mg, 0.36 mmol), and a catalytic amount of *p*-benzosulfonic acid were added to a 250-mL Schlenk flask equipped with a magnetic stir bar. This initial mixture was pumped dry under vacuum. Then, freshly distilled toluene/ethyl acetate/THF (3:1:1) mixture (150 mL) was charged into the flask under an argon atmosphere. The flask was attached to a Soxhlet extractor filled with oven-dried 4 Å molecular sieves. The reaction mixture was refluxed overnight. After the heating stopped, the dark, golden-brown solution was filtered by using a cannula to a second Schlenk flask equipped with a magnetic stir bar. The resulting imine solution was hydrogenated by using the general reduction method. The final solution was first washed with DI water then dilute $KHCO_3$ solution carefully to remove unreacted amino acid and phthalic acid. The organic phase was dried over Na_2SO_4, and the solution was concentrated by rotorvap. The final crude was crashed out with hexanes, first washed thoroughly with toluene (6×25 mL) for six cycles until the toluene becomes colorless, then washed with methanol (5×20 mL) for another five cycles to remove any residual amino acid precursors. The final product was dried in vacuuo. Final product: 14.1 mg (8%). MALDI-TOF MS calculated for $C_{73}H_{22}N_2O_3$ [M^+], 976.2, found 976.7.

N-Boc-C_{60}-Lys-OH (3): Bucky ketone (400 mg, 0.5 mmol), Ac-Lys(4-NH_2)-OMe.HCl (400 mg, 1.7 mmol), and a catalytic amount of *p*-benzosulfonic acid were added to a 500-mL Schlenk flask equipped with a magnetic stir bar. This initial mixture was pumped dry under vacuum. Then freshly distilled toluene/ethyl acetate/THF (6:1:1) mixture (400 mL) was charged into the flask under an argon atmosphere. The flask was attached to a Soxhlet extractor filled with oven-dried 4 Å molecular sieves. The reaction mixture was refluxed overnight. After the heating stopped, the dark, golden-brown solution was filtered by using a cannula to a second Schlenk flask equipped with a magnetic stir bar. The resulting buckyimine solution was hydrogenated following the general reduction method. The final solution was first washed with DI water, then dilute $KHCO_3$ solution carefully to remove unreacted amino acid and phthalic acid. The organic phase was dried over Na_2SO_4, and the resulting solution was concentrated on rotorvap. The final crude was crashed out with hexanes, first washed thoroughly with toluene (6×25 mL) until the toluene is colorless, then washed with methanol (5×20 mL) to remove any residual amino acid precursors. The final precipitate was dried in vacuum to yield 32.5 mg (6%) final product. MALDI-TOF MS, calculated for $C_{75}H_{28}N_2O_4$ [M^+], 1020.2, found 1019.8.

N-Boc-C_{60}-Lys-OMe (4): Bucky ketone (240 mg, 0.18 mmol), Ac-Lys(4-NH_2)-OMe (95 mg, 0.36 mmol), and a catalytic amount of *p*-benzosulfonic acid were added to a 250-mL Schlenk flask equipped with a magnetic stir bar. This initial mixture was pumped dry under vacuum. Then, freshly distilled toluene/ethyl acetate/THF (3:1:1) mixture (150 mL) was charged into the flask under an argon atmosphere. The flask was attached to a Soxhlet extractor filled with oven-dried 4 Å molecular sieves. The reaction mixture was refluxed overnight. After the heating stopped, the dark, golden-brown solution was filtered by using a cannula to a second Schlenk flask equipped with a magnetic stir bar. The resulting buckyimine solution was hydrogenated following the general reduction method. The final solution was first washed with DI water then dilute $KHCO_3$ solution to carefully remove unreacted amino acid and phthalic acid. The organic phase was dried over Na_2SO_4, and the resulting solution was concentrated by rotorvap. The final crude was crashed out with hexanes, first washed thoroughly with toluene (6×25 mL) until the toluene is colorless, then washed with MeOH (5×20 mL) for another five cycles to remove any residual amino acid precursors. The final product was dried in vacuum. Final product: 118.2 mg (64%). UV/Vis: λ_{max} (CH_2Cl_2) = 253, 325, 426 nm; MALDI-TOF MS, calculated for $C_{76}H_{30}N_2O_4$ [M^+], 1034.2, found 1035.0, 978.1.

C_{60}-phenylthiol (5): Bucky ketone (400 mg, 0.5 mmol), *p*-thiolaniline (360 mg, 2.2 mmol), and a catalytic amount of *p*-benzosulfonic acid were added to a 500-mL Schlenk flask equipped with a magnetic stir bar. This initial mixture was pumped dry under vacuum. Then, freshly distilled toluene (400 mL) was charged into the flask under an argon atmosphere. The flask was attached to a Soxhlet extractor filled with oven-dried 4 Å molecular sieves. The reaction mixture was refluxed overnight. After the heating stopped, the dark, golden-brown solution was filtered via cannula to a second Schlenk flask equipped with a magnetic stir bar. The resulting imine solution was hydrogenated following the general reduction method. The final solution was first washed with DI water, then dilute $KHCO_3$ solution to carefully remove unreacted 4-thiolaniline and phthalic acid. The organic phase was dried over Na_2SO_4 and the resulting solution was concentrated under vacuum. The resulting solid was dissolved in minimum amount CS_2 then loaded to a silica gel flash column. The column was first eluted with hexane/toluene (4:1) to remove any C_{60} impurity, and then eluted with toluene/hexane (4:1) to harvest the final product. Final product: 81.8 mg (18%). ^{1}H NMR [400 MHz, [D_8]toluene/CS_2 (1:1)]: δ = 7.12 (d, J(H,H) = 8.6 Hz, 2H), 6.47 (d, J(H,H) = 8.6 Hz, 2H), 4.56 (m, 1H), 4.11 (m, 1H), 3.41 (dd, J(H,H) = 4.2, 13.6 Hz, 1H), 3.39 (dd, J(H,H) = 4.2, 13.6 Hz, 1H), 3.10 (m, 2H), 2.99 (ddd, J(H,H) = 4.0, 4.9, 13.7 Hz, 1H), 2.20 ppm (qd, J(H,H) = 4.6, 10.2 Hz, 1H); UV/Vis: λ_{max} (CH_2Cl_2) = 256, 306, 322, 429 nm; MALDI-TOF MS, calculated for $C_{70}H_{13}NS$ [M^+], 899.1, found 898.5.

C_{60}-phenylbutyric acid (6): Bucky ketone (240 mg, 0.3 mmol), 4-(4-NH_2-phenyl)butyric acid (200 mg, 1.1 mmol), and a catalytic amount of *p*-benzosulfonic acid was added to a 500-mL Schlenk flask equipped with a magnetic stir bar. This initial mixture was pumped dry under vacuum. Then, freshly distilled toluene/THF (7:1) solvent mixture (400 mL) was charged into the flask under an argon atmosphere. The flask was attached to a Soxhlet extractor filled with oven-dried 4 Å molecular sieves. The reaction mixture was refluxed overnight. After the heating stopped, the dark, golden-brown solution was filtered by using a cannula to a second Schlenk flask equipped with a magnetic stir bar. The resulting buckyimine solution was hydrogenated following the general reduction method. The final solution was first washed with DI water, and then dilute $KHCO_3$ solution to carefully remove unreacted 4-(4-NH_2)-phenylbutyric acid and phthalic acid. The organic phase was dried by Na_2SO_4 and the resulting solution was concentrated by evaporation. The resulting concentrated solution was then loaded to a dry silica gel column. The column was first eluted with toluene to remove C_{60} impurities, and then eluted with toluene/ethyl acetate/THF (100:8:2) to harvest 115 mg (40%) of final product. ^{1}H NMR (400 MHz, [D_8]toluene/[D_8]THF/[D_7]DMF/$CDCl_3$): δ = 6.90 (d, J(H,H) = 6.6 Hz, 2H), 6.68 (d, J(H,H) = 6.6 Hz, 2H), 4.70 (m, 1H), 3.62 (dt, J(H,H) = 4.3, 13.0 Hz, 2H), 3.31 (dd, J(H,H) = 4.9, 13.5 Hz, 1H), 3.12 (m, 3H), 2.92 (td, J(H,H) = 4.2, 13.6 Hz, 1H), 2.38 (t, J(H,H) = 7.5 Hz, 2H), 2.10 (t, J(H,H) = 7.5 Hz, 2H), 1.75 ppm (p, J(H,H) = 7.5 Hz, 2H); UV/Vis: λ_{max} (CH_2Cl_2) = 256, 303, 322, 428 nm; MALDI-TOF MS, calculated for $C_{74}H_{19}NO_2$ [M^+], 953.1, found 953.4.

C_{60}-phenylamine-N-Boc (7): Bucky ketone (320 mg, 0.4 mmol), N-Boc-4-aminoaniline (260 mg, 1.2 mmol), and a catalytic amount of *p*-benzosulfonic acid was added to a 500-mL Schlenk flask equipped with a magnetic stir bar. This initial mixture was pumped dry under vacuum. Then, freshly distilled toluene/THF (7:1) solvent mixture (400 mL) was charged into the flask under an argon atmosphere. The flask was attached to a Soxhlet extractor filled with oven-dried 4 Å molecular sieves. The reaction mixture was refluxed for three days. After the heating stopped, the dark, golden-brown solution was filtered by using a via cannula to a second Schlenk flask equipped with a magnetic stir bar. The resulting buckyimine solution was hydrogenated following the general reduction method. The final solution was first washed with DI water, and then dilute $KHCO_3$ solution to carefully remove any unreacted N-Boc-4-aminoaniline and phthalic acid. The organic phase was dried over Na_2SO_4, and the resulting solution was concentrated by rotorvap to remove THF. The resulting concentrated solution was then loaded to dry silica gel column. The column was first eluted with toluene to remove C_{60} impurities, and then eluted with toluene/ethyl acetate (100:5) to harvest the final product of 105 mg (26%). ^{1}H NMR (400 MHz, [D_8]toluene/[D_8]THF): δ = 7.98 (s, 1H), 7.33 (s, 2H), 6.95 (d, J(H,H) = 7.1 Hz, 2H), 4.92 (m, 1H), 4.73 (m, 1H), 3.64 (dt, J(H,H) = 4.3, 13.0 Hz, 1H), 3.48 (dd, J(H,H) = 4.9, 13.5 Hz, 1H), 3.36 (dd, J(H,H) = 4.0, 10.7 Hz, 1H), 3.19 (m, 1H), 3.01 (td, J(H,H) = 4.0, 10.9 Hz, 1H), 1.37 ppm (s, 9H); ^{13}C{^{1}H} NMR: δ = 158.63, 158.07, 157.71, 157.53, 153.60, 148.22, 148.19, 147.01, 146.94, 146.77, 146.54, 146.45, 146.41,146.31, 146.00, 145.96, 145.91, 145.28, 143.78, 143.74, 143.65, 143.51, 143.08, 142.72, 142.67, 142.61, 142.18, 142.13, 142.10, 140.82, 140.68, 136.71, 136.41, 135.52, 135.30, 131.22, 127.71, 114.08, 64.87, 64.16, 49.17, 41.86, 35.82, 31.28, 26.83 ppm; UV/Vis: λ_{max} (CH_2Cl_2) = 255, 303, 325, 430 nm; MALDI-TOF MS, calculated for $C_{75}H_{20}N_2O_2$ [M^+], 980.2, found 981.4.

C_{60}-phenylamine (8): C_{60}-Phenylamine-Boc (**7**) (50 mg, 0.05 mmol) was mixed with TFA (5 mL) and sonicated for 2 h in a 25-mL scintillation vial. Then hexanes were added to crash and wash the final product. The final product of 45 mg (99%) was obtained after drying in vacuuo. MALDI-TOF MS, calculated for $C_{70}H_{14}N_2$ [M^+], 882.1 found 878.6. UV/Vis: λ_{max}(CH_2Cl_2) = 254, 305, 321, 429 nm.

C_{60}-di-ketone (9): C_{60} (1 g, 1.39 mmol) was pumped dry under vacuum, and then dissolved in freshly distilled toluene (400 mL) under argon and refluxed for 1 h to achieve maximum dissolution. The solution was cooled down to room temperature under inert atmosphere, and 2-trimethylsiloxy-1, 3-butadiene (236 mg, 1.42 mmol) in dry toluene (50 mL) was added in one portion. Afterwards, the reaction mixture was refluxed for 30 h and stirred at room temperature overnight. The final reaction mixture was dried under vacuum and the residue dissolved in a minimum amount of CS_2. The concentrated CS_2 solution was loaded onto a silica gel flash column and let stand for at least 12 h while covered with aluminum foil. This long duration sitting procedure is very important for the cleavage of trimethylsiloxyl group. The column was first eluted with hexanes/toluene (4:1) to remove unreacted C_{60}. The first dark brown band eluted with toluene produced mono C_{60} ketone (500 mg). MALDI-TOF calculated for $C_{64}H_6O$ [M^+], 790.0, found 790.0. The second dark brown band eluted with toluene/ethyl acetate gave isomers of C_{60}-di-ketone of 112 mg. UV/Vis: λ_{max} (CH_2Cl_2) = 244, 312 nm; MALDI-TOF calculated for calculated for $C_{68}H_{12}O_2$ [M^+], 860.1, found 860.0.

C_{60}-di-Phenylamine-Boc (10): Bis-bucky ketone (344 mg, 0.4 mmol), N-Boc-4-aminoaniline (500 mg, 2.4 mmol), and a catalytic amount of *p*-benzosulfonic acid was added to a 500-mL Schlenk flask equipped with a magnetic stir bar. This initial mixture was pumped dry under vacuum. Then, freshly distilled toluene/THF (7:2) solvent mixture (400 mL) was charged into the flask under an argon atmosphere. The flask was attached to a Soxhlet extractor filled with oven-dried 4 Å molecular sieves. The reaction mixture was refluxed for three days. After the heating stopped, the dark, golden-brown solution was filtered by using a cannula to a second Schlenk flask equipped with a magnetic stir bar. The resulting buckyimine solution was hydrogenated following the general reduction method. The final solution was first washed with DI water, and then dilute $KHCO_3$ solution to carefully remove any unreacted N-Boc-4-aminoaniline and phthalic acid. The organic phase was dried over Na_2SO_4, and the resulting solution was concentrated on rotorvap to remove THF. The resulting concentrated solution was then loaded onto a dry silica gel column. The column was first eluted with toluene to remove C_{60} impurity, and then eluted with toluene/ethyl acetate (100:8) to harvest the final product of 158 mg (32%). UV/Vis: λ_{max} (CH_2Cl_2) = 246, 260, 308 nm; MALDI-TOF MS, calculated for $C_{90}H_{44}N_4O_4$ [M^+], 1244.2, found 1244.0.

C_{60}-di-phenylamine (11): C_{60}-di-phenylamine-N-Boc (**10**) (138 mg, 0.13 mmol) was mixed with TFA (8 mL) and sonicated for 2 h in a 25-mL scintillation vial. Then hexanes were added to crash and wash the final product. 130 mg (96%) of the final product was obtained after drying in vacuuo. UV/Vis: λ_{max} (CH_2Cl_2) = 241, 270, 305 nm; MALDI-TOF MS, calculated for $C_{80}H_{28}N_4$ [M^+], 1044.2, found 1043.8.

Coupling of Fmoc-C_{60}-Phe-OH with NH_2-Gly-OEt: Compound **1c** (26 mg, 0.022 mmol) was mixed with NH_2-Gly-OEt (154 mg, 0.1 mmol) dissolved in 4:1 DCM/DMF (5 mL). HBTU (45 mg, 0.1 mmol) coupling reagents and a couple of drops NEt_3 were added thereafter. The solution was sonicated for 2 h. The solution was concentrated first and then precipitated by the addition of Et_2O (30 mL), resulting a brown solid, which was separated centrifuge (4400 rpm for 30 min.) and washed by MeOH (2×25 mL). MALDI-TOF MS (**12**) calculated 1161 [M^+], Found 1162 [M^+ + H], 1184 [M^+ + Na].

Baa-(Lys)$_9$-CO_2H (13): The couplings of first 9 residues of Fullerene peptide **13** were carried out on an automated APEX 396 Multiple Peptide Synthesizer (Advanced ChemTech) under nitrogen flow. Fmoc-Lys(Boc)-Wang resin (235 mg, 0.15 mM)was used as solid phase. Each coupling uses fourfold amino acid excess, and HBTU, HOBt as activators, and DIEA as base in a 1:1:1:3 ratio. Fmoc deprotection was performed using 25% perperidine in DMF solution. After the deprotection of the eighth residue (Glu) was finished, one sixth of the resin was moved out to a 25-mL fritted glass tube, swollen with DMF and a threefold excess of N-Boc-Baa (157 mg, 0.15 mmol) was dissolved in DMF/DCM (2:1, 9 mL). The Boc-Baa solution was first activated with PyBOP/HOBt/DIEA (1:1:1:3) for 2 min. The activated N-Boc-Baa was mixed with the resin in the fritted glass tube, and shaken on an automated shaker for one day at room temperature. Then the resin was washed thoroughly with DMF and DCM to remove unreacted N-Boc-Baa. The final peptide was cleaved twice from the solid support using TFA/TIPS/H_2O (98:1:1, 10 mL) for 4 h and 18 h. The crude fraction were washed with Et_2O and lyophilized to remove TFA. RP-HPLC purification was carried out on a Phenomenex Luna C5 column using an isocratic gradient of A: 0.1% TFA in water, and B: 0.1% TFA in 2-propanol, 70% B, at 5.0 mL min^{-1} flow rate. The elution time was 27 min. After purification 37.6 (36%) mg were recovered. MALDI-MS: m/z 2109 [M^+ + H], found 2109.

Baa-Lys(FITC)-(Lys)$_8$-CO_2H (14): The solid-phase synthesis of fullero-peptide **14** was carried out as described for fullero-peptide **13**, except that after the Lys_8 sequence was completed, a Lys(Mtt) residue was coupled to the end. After the Fmoc deprotection of Lys(Mtt) was finished, one sixth of the resin was moved out to a 25 mL fritted glass tube, swollen with DMF. A threefold excess of N-Boc-Baa (157 mg, 0.15 mM) was then dissolved in DMF/DCM (2:1, 9 mL) in a glass vial. The N-Boc-Baa solution was first activated with PyBOP/HOBt/DIEA (1:1:1:3) for 2 min, then mixed with the resin in the fritted glass tube, and shaken on an automated shaker for one day at room temperature. Then the resin was washed thoroughly with DMF and DCM to remove any unreacted N-Boc-Baa. Prior to the addition of FITC fluorescence label, the resin was washed with DCM for complete removal of DMF. To achieve the maximum cleavage of Mtt protecting group, the resin was shrunk with MeOH twice. Then the resin was treated three times with 1% TFA and 5% TIPS in DCM for 2 min. The resin was washed again with DCM thoroughly, and swelled in DMF for 1 h. Afterwards the resin was shaken with a solution of FITC (65 mg) in DMF (8 mL) and DIPEA (130 mL) overnight. At the end of the synthesis, the FITC labeled fullerene peptides was washed repeatedly with DMF, DCM, and shrunk with MeOH. The resin was thoroughly dried over Driete in vacuuo overnight. The Cleavage of the peptide was achieved with TFA/TIPS/thiolanisole/H_2O (92.5:2.5:2.5:2.5) cocktail for 4 h. After filtration, the peptide solution was concentrated by Rotavap at room temperature and precipitated with cold diethyl ether. The crude was washed with Et_2O two more times and.

After centrifugation of the final wash, it was frozen and lyophilized. RP-HPLC purification was carried out on a Phenomenex Luna C5 column using an isocratic gradient of A: 0.1% TFA in water, and B: 0.1% TFA in isopropanol, 70% B, at 5.0 mL min^{-1} flow rate. The elution time was 28 min. After purification 54.2 mg (43.4%) were recovered. MALDI-MS: *m*/*z* calculated 2496 [M^+], 2107, [M^+-FITC] found 2496, 2107.

Baa-(Glu)$_4$-(Gly)$_3$-Ser-CO$_2$H (15): The solid-phase synthesis of fullero-peptide **15** was carried out as described for fullero-peptide **13**. The final peptide was cleaved twice from the solid support using TFA/TIPS/H_2O (98:1:1, 10 mL) for 4 h and 18 h. The crude fractions were washed with Et_2O and lyophilized to remove TFA. RP-HPLC purification was carried out on a Phenomenex Luna C5 column using an isocratic gradient of A: 0.1% TFA in water, and B: 0.1% TFA in IPA, 70% B, at 5.0 mL min^{-1} flow rate. The elution time was 43 min. After purification 21.8 mg (25%) were recovered. MALDI-MS: *m*/*z* 1752 [M^++Na], found 1752.

Baa-(Glu)$_4$-(Gly)$_3$-Ser-Cys-OH (16): The solid-phase synthesis of fullero-peptide **16** was carried out as described for fullero-peptide **13**. The final peptide was cleaved twice from the solid support using TFA/TIPS/H_2O (98:1:1, 10 mL) for 4 h. The crude fractions were precipitated and washed with Et_2O and lyophilized to remove TFA. RP-HPLC purification was carried out on a Phenomenex Luna C5 column using an isocratic gradient of A: 0.1% TFA in water, and B: 0.1% TFA in IPA, 70% B, at 5.0 mL min^{-1} flow rate. The elution time was 37 min. After purification 8.0 mg (9%) were recovered. MALDI-MS: *m*/*z* 1889 [M^+], 1912 [M^++Na], found 1889, 1911.

Baa-Arg-Gln-Ile-Lys-Ile-Trp-Phe-Gln-Asn-Arg-Arg-Met-Lys-Trp-Lys-Lys-OH (Baa-Penetratin, 17): The solid-phase synthesis of fullero-peptide **17** was carried out as described for fullero-peptide **13**. The final peptide was cleaved twice from the solid support using TFA/TIPS/H_2O (98:1:1, 10 mL) for 4 h. The crude fractions were precipitated and washed with Et_2O and lyophilized to remove TFA. RP-HPLC purification was carried out on a Phenomenex Luna C5 column using an isocratic gradient of A: 0.1% TFA in water, and B: 0.1% TFA in isopropanol, 70% B, at 5.0 mL min^{-1} flow rate. The elution time was 33 min. After purification 58.7 mg (36.9%) were recovered. MALDI-MS: *m*/*z* calculated 3184 [M^++H], found 3184.

Glu-Ile-Ala-Gln-Leu-Glu-Baa-Glu-Ile-Ser-Gln-Leu-Glu-Gln-NH$_2$ (18): The coupling of the first six residues was carried out on an automated APEX 396 Multiple Peptide Synthesizer (Advanced ChemTech) under nitrogen flow using a rink amide resin (430 mg, 0.3 mM) as the solid phase. Each coupling uses four-fold excess of the amino acid, and HBTU, HOBt as activators and DIEA as base in a 1:1:1:3 ratio. Fmoc deprotection was performed using 25% piperidine in DMF solution. After the deprotection of the sixth residue (Glu), one sixth of the resin (ca. 0.05 mM) was placed in a 25-mL fritted glass tube, and swollen with DMF (ca. 10 mL). A threefold excess of Fmoc-Baa was dissolved in DMF/DCM (2:1) (9 mL) in a second glass vial. The Fmoc-Baa solution was first activated with PyBOP/HOBT/DIEA (1:1:1:2) for 2 min, then mixed with the resin in the fritted glass tube, and shaken on an automated shaker for one day at room temperature. Then the resin was washed thoroughly with DMF and DCM to remove unreacted Fmoc-Baa, and retransferred in the automated synthesizer reactor. Fmoc removal was performed in the synthesizer, using a 5% DBU solution in DMF. The subsequent amino acid couplings were accomplished using the conditions described above. The final peptide was cleaved from the solid support by washing with TFA/TIPS/H_2O (98:1:1, 10 mL) for 4 h and a second time for 18 h. The crude fractions were washed with Et_2O and lyophilized to remove TFA. Purification was carried out on an Varian C4 column using a gradient of TFA (0.1%) in H_2O to TFA in IPA (0.1%) over 75 min at flow rate of 5.0 mL min^{-1}. The elution time was 57 min. Yield: 8.5 mg (6.8%). MALDI-MS: *m*/*z,* calculated 2488 [M^++Na], found 2489.

Baa-Glu-Ile-Ala-Gln-Leu-Glu-Tyr-Glu-Ile-Ser-Gln-Leu-Glu-Gln-NH$_2$ (Baa-2HP, 19): The solid-phase synthesis of fullero-peptide **19** was carried out as described for fullero-peptide **13**. The final peptide was cleaved twice from the solid support using TFA/TIPS/H_2O (95:2.5:2.5, 10 mL) for 4 h and 18 h. The crude fractions were washed with Et_2O and lyophilized to remove TFA. RP-HPLC purification was carried out on a Phenomenex Luna C5 column using an isocratic gradient of A: 0.1% TFA in water, and B: 0.1% TFA in IPA, 70% B, at 5.0 mL min^{-1} flow rate. The elution time was 41 min. After purification 20.6 mg (15.4%) were recovered. MALDI-MS: *m*/*z* calculated 2671 [M^++Na], found 2671.

Baa-Glu-Ile-Ala-Gln-Leu-Glu-Tyr-Glu-Ile-Ser-Gln-Leu-Glu-Gln-Glu-Ile-Gln-Ala-Leu-Glu-Ser-NH$_2$ (Baa-3HP, 20): The solid-phase synthesis of fullero-peptide **20** was carried out as described for fullero-peptide **13**. The final peptide was cleaved twice from the solid support using TFA/TIPS/H_2O (95:2.5:2.5, 10 mL) for 4 h and 18 h. The crude fractions were washed with Et_2O and lyophilized to remove TFA. RP-HPLC purification was carried out on a Phenomenex Luna C5 column using an isocratic gradient of A: 0.1% TFA in water, and B: 0.1% TFA in IPA, 70% B, at 5.0 mL min^{-1} flow rate. The elution time was 42 min. After purification 8.8 mg (8.7%) were recovered. MALDI-MS: *m*/*z,* calculated 3399 [M^++2H], 3421 [M^++Na], found, 3400, 3421.

Synthesis of C_{70} ketone (21): The C_{70}-ketone was prepared using the same revised method as C_{60} ketone. C_{70} (1.00 g, 1.19 mmol) was dissolved in toluene (500 mL). The dark red solution was refluxed for 2 h followed by addition of 2-trimethylsiloxyl-1,3-butadiene (0.202 g). Yield: 600 mg (55.0%). MALDI-TOF MS calculated for $C_{74}H_6O$ [M]$^+$, 910.0, found 909.6. UV/Vis: $\lambda_{max}(CH_2Cl_2)$=234, 304, 339, 392, 458, 529 nm.

Synthesis of N-Boc-C_{70}-Phe-OH (22): The N-Boc-C_{70}-Phe-OH was prepared using the same method as its C_{60} analogue. C_{70}-ketone (200 mg, 0.2 mmol) reacted with N-Boc-Phe-OH (168 mg, 0.6 mmol) to produce **22** (118 mg, 50.3%) in three days. ^{1}H NMR (500 MHz, [D_8]toluene/[D_7]DMF) for major isomer: δ=7.27 (d, J(H,H)=8.3 Hz, 1H), 6.86 (d, J(H,H)=8.3 Hz, 2H), 6.32 (dd, J(H,H)=7.9, 6.4 Hz, 1H), 4.64 (ddd, J(H,H)=7.9, 7.9, 5.0 Hz, 1H), 4.42 (m, 1H; -CH(hexagonal ring)), 3.29 (dd, J(H,H)=13.9, 5.0 Hz, 1H), 3.16 (m, 1H), 3.14 (ddd, J(H,H)=13.9, 7.9, 6.4 Hz, 1H), 3.03 (m, 1H), 2.87 (m, 1H), 2.69 (m, 1H), 2.19 (m, 1H), 2.14 (m, 1H), 1.44 ppm (s, 9H; C(CH_3)$_3$); ^{13}C{^{1}H} NMR (125.8 MHz, [D_8]toluene/[D_7]DMF). At least 64 signals (italics) can be reasonably attributed to C_{70} sp^2 signals from the major isomer. See Figure 12 for other assignments: δ=174.32, 156.03, *155.79, 155.52, 151.81, 151.79, 151.75, 151.73, 151.71, 151.69, 151.09, 151.03, 151.00, 150.99, 150.26, 150.25, 150.22, 150.20, 150.17, 150.16, 150.13, 149.75, 149.74, 149.73, 149.72, 149.34, 149.32, 149.18, 149.14, 148.872, 148.866, 147.79, 147.73, 147.44, 147.43, 147.36, 147.35, 147.31, 147.17,* 146.97, *146.94, 146.76, 146.75, 145.98, 145.96, 143.49, 143.42, 143.36, 143.27, 143.15, 143.07, 143.00, 140.99, 140.69, 140.62, 140.04, 136.66, 134.31, 134.28, 134.23, 134.21, 131.73, 131.66, 131.65, 131.63, 131.61, 131.58,* 130.86, 126.14, 113.77, 78.55, 57.78, 56.14, 55.21, 46.92, 40.80, 37.48, 31.64, 30.19, 28.52 ppm; UV/Vis: λ_{max}(CH_2Cl_2, nm)=233, 308, 341, 394, 454 nm; MALDI-TOF MS calculated for $C_{88}H_{26}N_2O_4$ [M^+], 1174.2, found 1172.8.

Synthesis of C_{70}-Phe-OH (23): N-Boc-C_{70}-Phe-OH (20 mg) was mixed with TFA (5 mL) and sonicated for 2 h in a 25-mL scintillation vial. The final product precipitated out of TFA as reaction proceeded. The final product was centrifuged out and washed with hexanes and water. The final product was lyophilized. Yield 7.5 mg (41.0%). MALDI-TOF MS, calculated for $C_{83}H_{18}N_2O_2$ [M^+], 1074.1, found 1073.8.

Acknowledgements

Financial support for this work is provided by the Robert A. Welch Foundation. Funding toward the purchase of the 400 and 500 MHz spectrometers was provided by the National Science Foundation. We thank He Dong, Sergey Paramonov, Virany Yowono, and Lorenzo Aulisa for assistance with SPPS, and Yasuhiro Shirai from the group of Prof. James Tour for electrochemical measurements. We are grateful to CSixty Inc. for providing C_{60} samples and antioxidant activity measurement.

[1] H. W. Kroto, J. R. Heath, S. C. O'Brien, R. F. Curl, R. E. Smalley, *Nature* **1985**, *318*, 162.
[2] E. Nakamura, H. Isobe, *Acc. Chem. Res.* **2003**, *36*, 807.
[3] K. M. Kadish, R. S. Ruoff, *Fullerenes: Chemistry, physics, and technology*, Wiley, New York, **2000**, p. 53.

[4] Y. N. Yamakoshi, T. Yagami, K. Fukuhara, S. Sueyoshi, N. Miyata, *J. Chem. Soc. Chem. Commun.* **1994**, 517.
[5] J. L. Atwood, G. A. Koutsantonis, C. L. Raston, *Nature* **1994**, *368*, 229.
[6] T. Andersson, K. Nilsson, M. Sundahl, G. Westman, O. Wennerström, *J. Chem. Soc. Chem. Commun.* **1992**, 604.
[7] L. Y. Chiang, J. B. Bhonsle, L. Wang, S. F. Shu, T. M. Chang, J. R. Hwu, *Tetrahedron* **1996**, *52*, 4963.
[8] G. A. Burley, P. A. F. Keller, S. G. Pyne, E. Ball, *J. Org. Chem.* **2002**, *67*, 8316.
[9] M. Maggini, G. Scorrano, A. Bianco, C. Toniolo, R. P. Sijbesma, F. Wudl, M. Prato, *J. Chem. Soc. Chem. Commun.* **1994**, 305.
[10] L. Gan, D. Zhou, C. Luo, H. Tan, C. Huang, M. Lu, J. Pan, Y. Wu, *J. Org. Chem.* **1996**, *61*, 1954.
[11] Y.-Z. An, J. L. Anderson, Y. Rubin, *J. Org. Chem.* **1993**, *58*, 4799.
[12] F. Pellarini, D. Pantarotto, T. Da Ros, A. Giangaspero, A. Tossi, M. Prato, *Org. Lett.* **2001**, *3*, 1845.
[13] A. Skiebe, A. Hirsch, *J. Chem. Soc. Chem. Commun.* **1994**, 335.
[14] J. Yang, A. R. Barron, *Chem. Commun.* **2004**, 2884.
[15] J. G. Rouse, J. Yang, A. R. Barron, N. A. Monteiro-Riviere, *Toxicol. in Vitro* **2006**, *20*, 1313.
[16] P. S. Ganapathi, S. H. Friedman, G. L. Kenyon, Y. Rubin, *J. Org. Chem.* **1995**, *60*, 2954.
[17] Y.-Z. An, C. B. Chen, J. L. Anderson, D. S. Sigman, C. S. Foote, Y. Rubin, *Tetrahedron* **1996**, *52*, 5179.
[18] C. Jehoulet, A. J. Bard, F. Wudl, *J. Am. Chem. Soc.* **1991**, *113*, 5456.
[19] P. M. Allemand, A. Koch, F. Wudl, Y. Rubin, F. Diederich, M. M. Alvarez, S. J. Anz, R. L. Whetten, *J. Am. Chem. Soc.* **1991**, *113*, 1050.
[20] L. B. Alemany, A. Gonzalez, W. E. Billups, M. R. Willcott, E. Ezell, E. Gozansky, *J. Org. Chem.* **1997**, *62*, 5771.
[21] L. B. Alemany, *Magn. Reson. Chem.* **1989**, *27*, 1065.
[22] H.-O. Kalinowski, S. Berger, S. Braun, *Carbon-13 NMR Spectroscopy*, Wiley, Chichester, **1988**.
[23] J. B. Stothers, *Carbon-13 NMR Spectroscopy*, Academic Press, New York, **1972**.
[24] A. Giangaspero, I. Zelensky, J.-P. Briand, M. Prato, *J. Am. Chem. Soc.* **2002**, *124*, 12543.
[25] L. A. Watanabe, M. P. I. Bhuiyan, B. Jose, T. Katob, N. Nishino, *Tetrahedron Lett.* **2004**, *45*, 7137.
[26] H. Dong, J. D. Hartgerink, *Biomacromolecules* **2006**, *7*, 691.
[27] B. Sitharaman, S. Asokan, I. Rusakova, M. S. Wong, L. J. Wilson, *Nano Lett.* **2004**, *4*, 1759.
[28] V. Georgakilas, F. Pellarini, M. Prato, D. M. Guldi, M. Melle-Franco, F. Zerbetto, *Proc. Natl. Acad. Sci. USA* **2002**, *99*, 5075.
[29] S. R. Wilson, Y. Hu, T. Zhu, R. Lebovitz, US Patent Application 20050130939.
[30] T. Gareis, O. Kothe, E. Beer, J. Daub, *Recent Advances in the Chemistry and Physics of Fullerenes and Related Materials 96-10*, *Vol. 3*, Electrochemical Society, **1996**, p. 1244.
[31] T. Gareis, O. Kothe, J. Daub, *Eur. J. Org. Chem.* **1998**, 1549.
[32] J. Yang, L. B. Alemany, A. R. Barron, submitted for publication.
[33] Y. Zhao, Y. Shirai, A. D. Slepkov, L. Cheng, L. B. Alemany, T. Sasaki, F. A. Hegmann, J. M. Tour, *Chem. Eur. J.* **2005**, *11*, 3643.

Received: August 16, 2006
Revised: October 20, 2006
Published online: January 19, 2007

